PHILIPS

APPLICATION BOOK

PHILIPS ELECTRONIC COMPONENTS AND MATERIALS

FAST RESPONSE PHOTOMULTIPLIERS

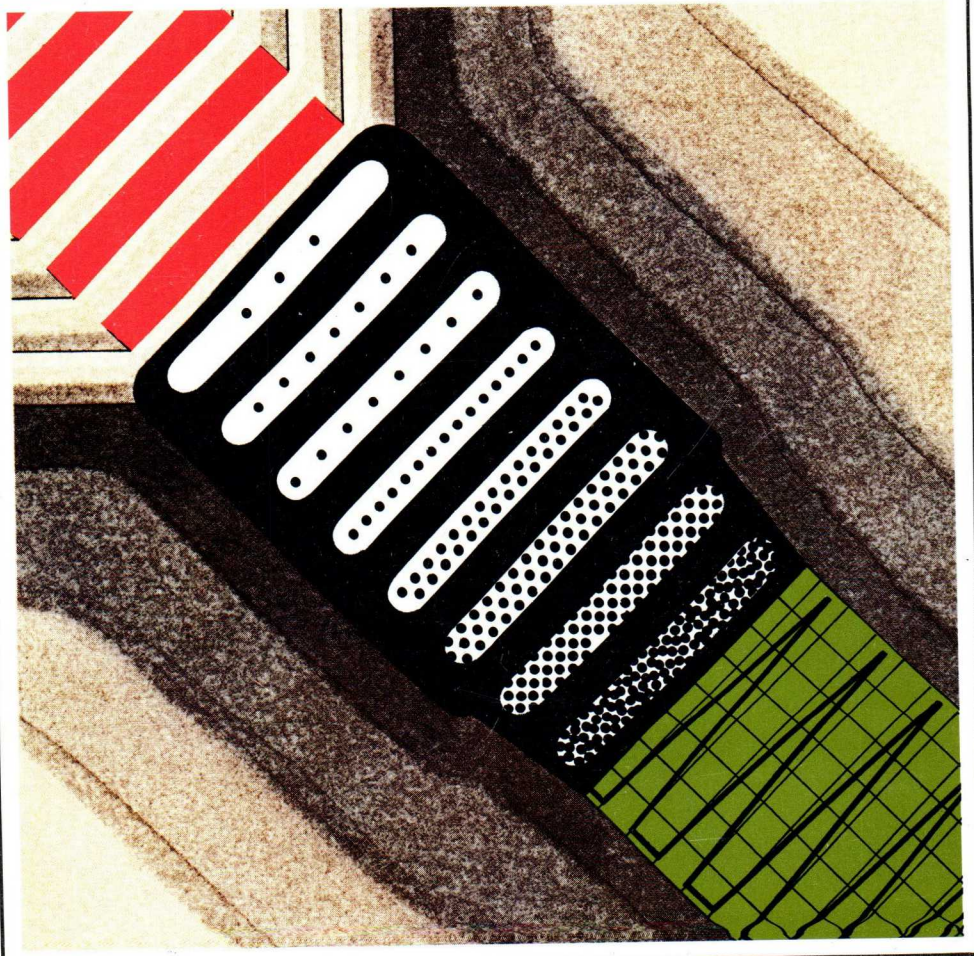

Fast Response Photomultipliers

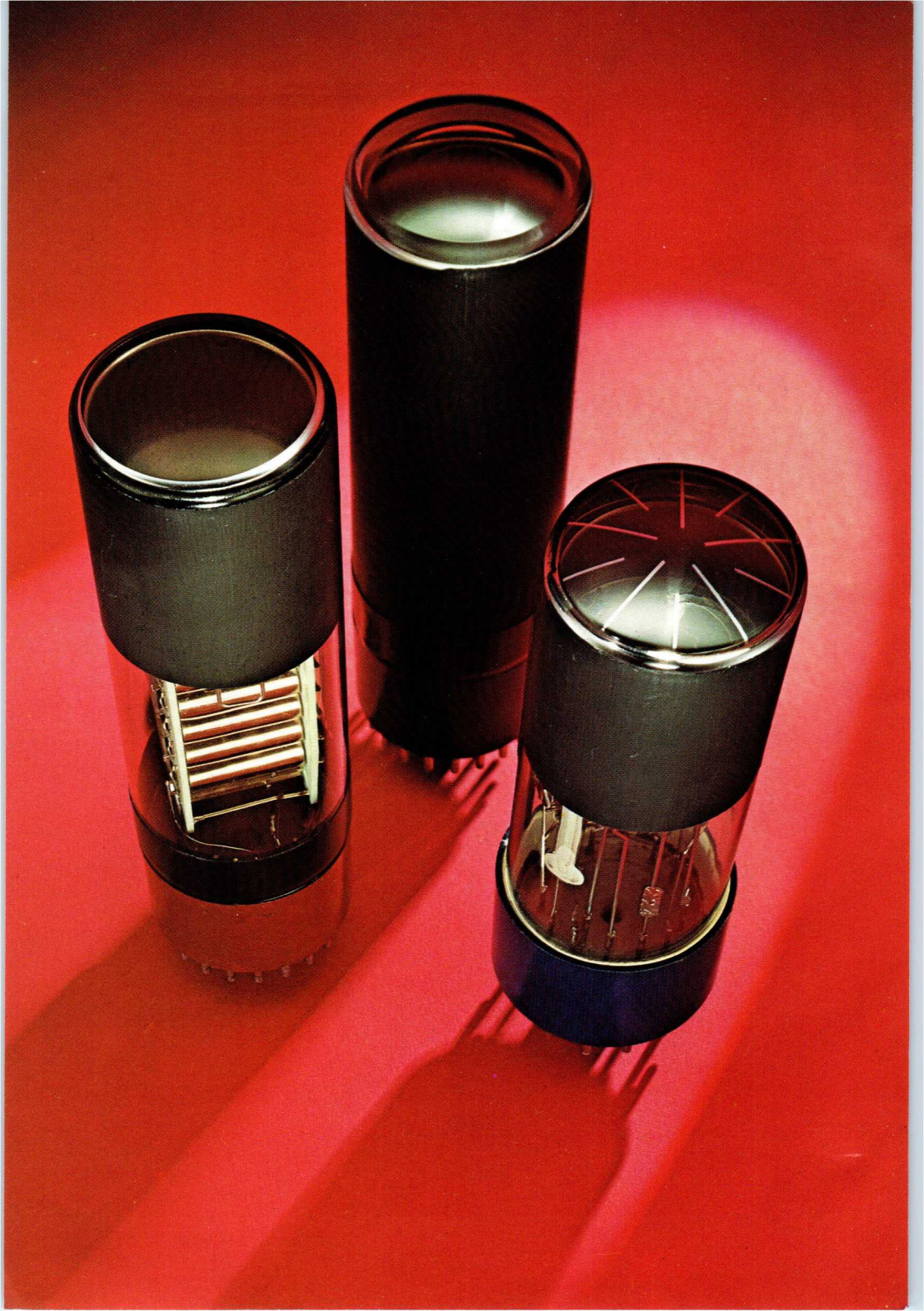

Fast Response Photomultipliers

Edited by

M. D. Hull., C. Eng., A.M.I.E.R.E.

PUBLICATIONS DEPARTMENT
ELECTRONIC COMPONENTS AND MATERIALS DIVISION

Contents

Acknowledgements

Acknowledgements are made to R.T.C. La Radiotechnique-Compelec, France, from whose publication "Tubes Photomultiplicateurs à Réponse Rapide" the information given in this book has been obtained; also to J. M. Schonkeren of the Central Applications Laboratory, Eindhoven, for his assistance in checking the text, and particularly the mathematics.

Foreword

The scope of research and development in nuclear physics has been increasing enormously of recent years, and this has led to a need for measuring techniques which are more and more precise and complex. The measuring instruments have had to be improved at the same time, to allow research workers to explore avenues which had been inaccessible hitherto owing to the limitations on the accuracy of measurement.

Photomultipliers, which are among the best detection instruments for research and experimentation in atomic physics today, have undergone continual improvements since they were first developed, as our knowledge of the underlying physical and technological processes improved. At the present time the properties of photomultipliers are approaching their theoretical limits; but progress in this field is still continuing.

A wide variety of photomultipliers has been developed to meet various specialized needs. Among the new types developed recently are photomultipliers of very high stability for use in particle or electromagnetic spectrometry, photomultipliers with very low noise specially designed for microactivity measurements, reinforced photomultipliers for space applications, and fast response photomultipliers with a very wide range of linearity which make it possible to measure phenomena that change very rapidly in time, or recur at very frequent intervals, in the domain of high-energy physics.

This book, which is devoted to fast response photomultipliers, illustrates the remarkable performance in terms of time and linearity which can be obtained from these instruments. In this respect, a fast response photomultiplier stimulated by a very short light pulse can give a current pulse whose rise time is of the order of a nanosecond; this property makes the photomultiplier the best wideband amplifier there is.

List of Main Symbols used in the Text

c	velocity of light
e	charge on an electron
E	electric field strength
f	frequency
Δf	bandwidth
F	focal length
g	focusing electrode; gain of a stage
G	overall gain; generating function
h	Planck's constant
I	direct current
I_a	anode current
I_k	cathode current
k	cathode
l	length of flight path
m	percentage modulation
n	positive whole number; refractive index
N_{ar}	anode radiant sensitivity
N_e	number of electrons
N_p	number of photons
N_s	number of signal pulses
p	momentum of particles
P	probability
Q	charge
S	dynode
t	time
u	velocity of particles in vacuo
V_s	inter-dynode voltage
W	kinetic energy of an electron

δ secondary emission coefficient

η_c collection efficiency

η_q quantum efficiency

λ wavelength

$\Delta\lambda$ bandwidth

σ standard deviation

σ^2 variance: $\sum_{n=0}^{\infty} P(n)(n-\bar{n})^2$

where $P(n)$ is the probability of obtaining the value n.
For a distribution obeying Poisson's Law:

$$P(n) = \frac{(\bar{n})^n e^{-\bar{n}}}{n!}$$

τ time

υ relative variance: $\dfrac{\sigma^2}{(\text{average value})^2} = \dfrac{\sigma^2}{(\bar{n})^2}$

ψ statistical variable defining pulse width

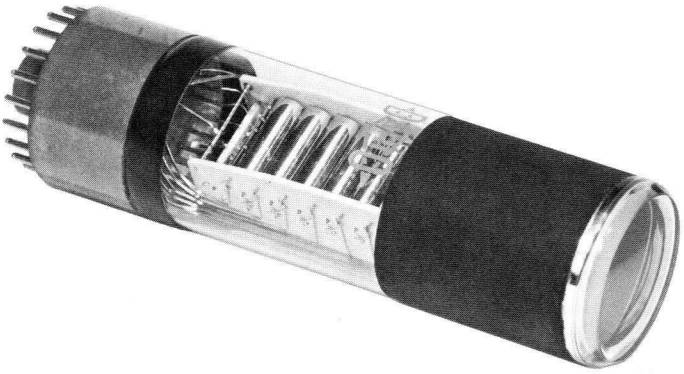

Fast response photomultiplier type 56AVP
(approx. half full size)

1 Introduction

Of recent years, physicists have felt the need to improve the response of photomultipliers so as to take full advantage of the brevity of the light pulses produced by scintillators. In certain substances, these light pulses only last a few nanoseconds, while the pulses of Cerenkov light produced by relativistic particles in transparent media are even shorter.

Such fast photomultipliers would make it possible to carry out a number of important measurements in nuclear physics, in particular the determination of the mean life of excited states in the nucleus by "fast coincidence" methods, or the determination of the velocity of high-energy particles by "time-of-flight" measurements.

Our laboratories have therefore developed new fast response photomultipliers with the following properties:

- very low fluctuation of the transit time of the electrons;
- high peak currents in low impedances (50 to 100 Ω);
- high gain (bearing in mind the small amounts of light incident on the photocathode);
- high quantum efficiency of the photocathode, which leads to less random fluctuation of pulse heights.

2 Principal Properties of the Photomultiplier

Before studying fast response photomultipliers in detail, a brief survey of the basic properties of photomultipliers is given here. A more detailed general treatment of the subject will be found in our Application Book "Photomultipliers".

2.1 Construction of a Photomultiplier

Fig. 2.1 shows the principles of construction of a photomultiplier.

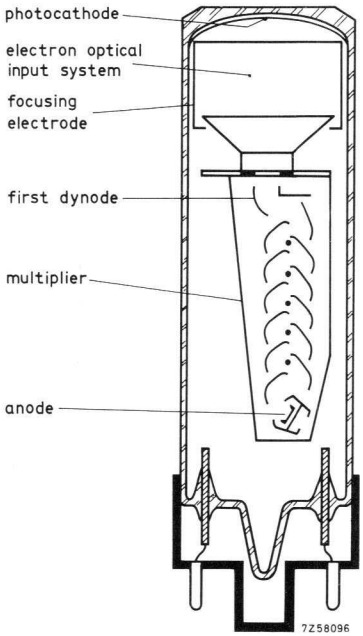

Fig. 2.1. Principal constructional details of a photomultiplier.

Briefly, a photomultiplier consists of:

- a photocathode, generally semi-transparent, deposited on the inner surface of an optically polished window. This photocathode converts a luminous flux of photons falling within its spectral sensitivity range into a flux of electrons emitted in vacuo.
- an electron-optical input system which concentrates the electrons coming from the photocathode as accurately as possible on the first dynode of the multiplier.
- a multiplier, consisting of a series of *dynodes*, which "multiplies" the electrons (initially emitted by the photocathode) by the emission of secondary electrons. The multiplier is terminated by a collector or anode, which receives the electron flux coming from the last dynode.

The above parts are contained in a sealed envelope, which is evacuated to obtain a pressure as low as possible. This is very important for the proper functioning of the photomultiplier, since both the photoemissive layer on the photocathode and the secondary-emission layers on the dynodes are very sensitive to gaseous or other contamination.

2.2 Principal Properties

2.2.1 The Photocathode

The quality of a photomultiplier depends in the first place on its photocathode. The principal characteristics of this electrode are its sensitivity, spectral response, homogeneity, and the level of the parasitic electron flux produced spontaneously (in the absence of any incident radiation).

For photometric applications, the sensitivity of the photocathode can be given in amperes per lumen (for white light of a specified composition[1]) or in amperes per watt (for monochromatic radiation). However, the sensitivity can also be expressed as a quantum efficiency, defined as the number of electrons emitted per 100 incident photons of given wavelength received by the photocathode.

The sensitivity of a photocathode depends not only on the characteristics of the photoemissive substance used, but also on the wavelength of the incident light. The curve giving the variation of the sensitivity of a photocathode with the wavelength of the incident photons is called the spectral response curve. The spectral response curves of the most widely used photocathodes are shown in Fig. 2.2, while Table 1 gives the principal characteristics of all the photoemissive layers in current use.

[1] White light with a colour temperature of 2854° K.

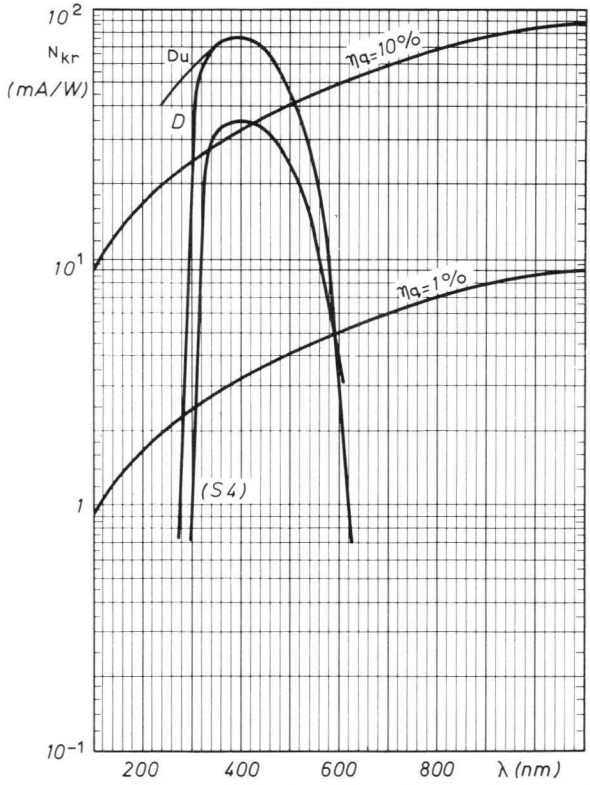

Fig. 2.2. (a) Spectral sensitivities of the main types of photocathodes used.
——— *glass window*

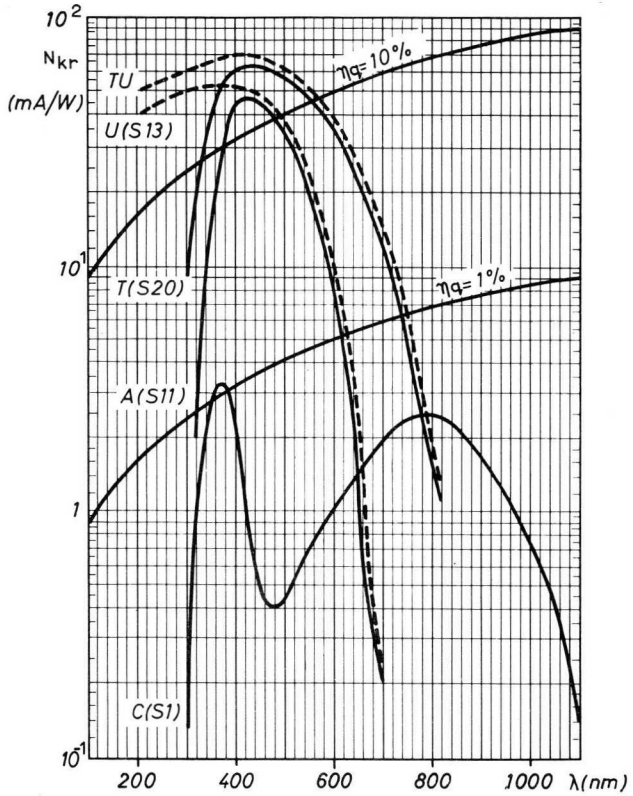

Fig. 2.2. (b) Spectral sensitivities of the main types of photocathodes used.
——— *glass window*
- - - - - - - *fused-quartz window, transparent to UV*

Table 1. Characteristics of the photoemissive layers most commonly used in photomultipliers

type of cathode	constituents	spectral response type	$\lambda_{(nm)}$ [1])	η_q (%)	N_{kr} (μA/lm) [2])	N_{kr} (mA/W) [3])
S1	Ag–O–Cs	C	800		25	2.5
S4	Sb–Cs		400	10	45	35
S11	Sb–Cs–O	A	440	15	65	55
S13	Sb–Cs–O on quartz	U	440	15	65	55
S20	Sb–Na–K–Cs	T	420	19	115	65
	Sb–Na–K–Cs on quartz	TU	420	19	115	65
bi-alkaline	Sb–K–Cs	D	400	22	50	75
	Sb–K–Cs on quartz	DU	400	22	50	75

[1]) Wavelength corresponding to the maximum sensitivity N_{kr} of the photoemissive layer (nm = nanometre = 10^{-9} m).
[2]) Sensitivity of the photoemissive layer for standard white light (colour temperature 2854° K).
[3]) Maximum sensitivity of the photoemissive layer.

No matter how high the amplification provided by the multiplier system (and it is very high), it is important that the sensitivity of the photocathode should be as high as possible. The emission of photoelectrons by the cathode is basically a statistical process; one photon will on average liberate a constant number of electrons from the cathode, but the actual value fluctuates about this mean. This fluctuation becomes less as the cathode sensitivity is increased. Any further amplification will also reproduce these fluctuations, which will appear in the final anode pulse. This is why the cathode should have as high a quantum efficiency as possible.

Now the light produced by the scintillator is not always produced in the same spot and will therefore affect different zones of the photocathode. This gives another possible cause of variation in the height of the output pulse, since the sensitivity of the photocathode may be expected to vary a certain extent from point to point. The *homogeneity* of the cathode is, therefore, another important characteristic which the manufacturer continually tries to improve with the aid of new production methods.

The homogeneity of a photocathode can be studied in a relatively simple manner with the aid of a very small spot of light which scans the useful surface of the photocathode diametrically. The variation of the photoelectric current as a function of the coordinates of the light spot can be displayed on an oscilloscope screen, and photographed. Fig. 2.3 shows records obtained in this way with different photocathodes.

Another important factor is the *dark current*, i.e. the signal obtained at the anode of the photomultiplier when no light at all falls on the photocathode.

A large part of this parasitic signal is due to the spontaneous emission of electrons by the various electrodes of the tube. The current in question is largely thermionic, emitted at the ambient temperature by the photocathode or dynodes by reason of their low work function. A typical photomultiplier type 56 AVP gives a dark current (expressed in terms of the current of the photocathode) of between 10^{-17} and 10^{-15} A/cm^2 at room temperature. This means that, in addition to the useful signal, from 60 to 6000 electrons will always be emitted (in a random manner) per square centimetre of photocathode surface per second. Cooling the photomultiplier reduces the dark current effectively, but to a variable extent.

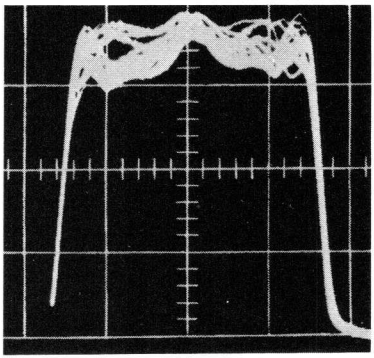

Good homogeneity

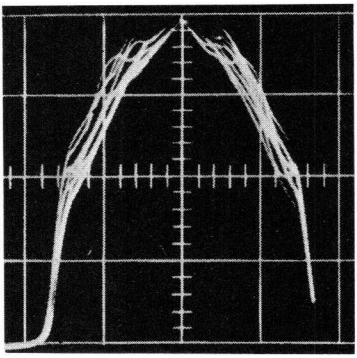

Poor homogeneity (lack of sensitivity at edges)

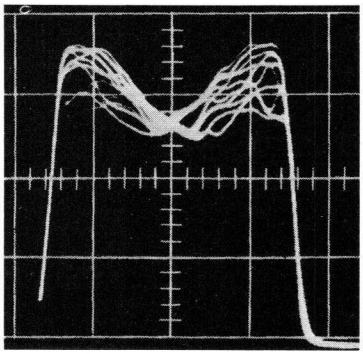

Poor homogeneity (lack of sensitivity at middle)

Fig. 2.3. Oscillograms demonstrating the homogeneity of the photocathode

2.2.2 Input Optics

The input optics comprises a system of electrodes which guides the electrons emitted by the photocathode to the active zone of the first dynode of the multiplier. Two requirements which tend to be incompatible have to be satisfied:

- efficient collection of the electron beams emitted by all parts of the photocathode;
- efficient transfer of the electrons from a region where the electrostatic field has rotational symmetry to one where the field has cylindrical symmetry.

The *collection efficiency* of the input optics, or the percentage of electrons emitted by the photocathode which it allows to reach the multiplier, is thus an important characteristic and should be as near as possible to 100%. A distinction is made here between the *mean* collection efficiency for the cathode as a whole, and the *local* efficiency of limited regions of the cathode. Type 56 AVP photomultipliers have a local efficiency of 80% or more at all points on the photocathode.

For many years, the input optics consisted simply of the photocathode and the first dynode of the multiplier, as this simplified control. However, it has been found recently that it is quite essential to add one or two intermediate electrodes to improve the accuracy of focusing of the electrons in space, which determines the collection efficiency, and what we may call the accuracy of focusing "in time" so as to avoid differences in transit time of the electrons between various parts of the system. This problem is of vital importance for fast response photomultipliers, as we shall see below.

2.2.3 The Multiplier

The multiplier, which is made up of a number of dynodes, starts off with a transition zone that is one of the most critical spots of the whole photomultiplier.

This zone generally comprises two or three dynodes whose cross-section differs from that of the rest of the dynodes in the "iterative" part of the multiplier. These first dynodes, with their special geometry, are there (apart from multiplication pure and simple) to adapt the form of the electron beam reaching the first dynode to provide the mean angle of incidence and the spread required by the iterative structure.

The *total amplification* provided by multiplier depends on the number of dynodes and the gain per stage, i.e. the ratio of the number of secondary

electrons received by dynode number (Sn + 1) and the number of electrons received by dynode number Sn.

The gain of a stage (g_i) can thus be written as the product of the secondary emission coefficient (δ_i) of the ith dynode and the collection efficiency ($\eta_{C(i)}$) between the ith stage and the next:

$$g_i = \delta_i \cdot \eta_{C(i)} .$$

Since the secondary emission effect is statistical in nature, and the number of electrons entering the multiplier is relatively small, it will be clear that the collection efficiency of each stage should be as close to 100% as possible and that the operating conditions should be chosen so as to maximize the gain per stage.

At each stage of the multiplier, we also get a problem similar to that mentioned above in connection with the input optics. This is to ensure that the transit times of the different electron trajectories differ as little as possible regardless of their point of departure and initial velocity. The different electrons should take the same time moving from one dynode to the next. This is a problem of electron optics, involving the profile of the dynodes and the potentials applied to them.

Parasitic effects produced in the tube, can lead to instability of operation. These effects are important as the HT voltage applied to the tube is higher. Apart from thermionic emission from the cathode and the dynodes, these effects include:

- ionization of the residual gas by the electrons, followed by the emission of secondary electrons from the cathode or the dynodes under the influence of the ions produced;
- field-effect emission (Schottky effect, or tunnel effect) from sharp points or cracks in the electrodes, soldered joints, etc;
- electroluminescence of various materials such as the dynodes themselves, the insulators, certain parts of the envelope, etc., under the influence of the electrons from the main flux or those produced by cold emission.

Summing up, the number of dynodes, their geometry and the potentials applied to them, should all be chosen so as to give the best possible combination of high gain, low dark current, good stability and uniform transit times for all electron trajectories.

To give the reader an idea of the quantities involved, if the overall gain is 10^6, the number of stages generally varies from 9 to 11, while with higher gains of 10^8 to 10^9 the number of stages may be as high as 14. The secondary emission coefficient of the dynodes is of the order of 3 to 5.

2.3 Limitations on Accuracy of Measurements

In nuclear physics, a photomultiplier is generally used, together with a scintillator, for one of the following applications: determination of the energy of a radiation, determination of the instant at which a particle is produced, or measurement of the time interval between two nuclear events.

The amount of charge collected at the output of a scintillation counter is proportional, to a first approximation, to the energy lost in the scintillator by the incident radiation. The energy measurements thus come down basically to measurement of a quantity of charge. However, the events taking place in a detector of this type between the moment when the particle enters the scintillator and the moment when the electric charge reaches the anode are stochastic in nature, and set a natural limit to the accuracy with which the energy can be measured. This limitation is due to the statistical fluctuations in the number of elementary charges received by the anode.

Statistical fluctuations limit the accuracy of time measurements in a similar way. Such measurements are based on the time at which a characteristic element of the anode pulse occurs (maximum amplitude, 50% point of rise time, centre of gravity of pulse, etc.). Now the time elapsing between the entry of the particle into the scintillator and the appearance of the characteristic element of the corresponding pulse is also subject to statistical fluctuations, and exhibits a certain spread about the mean response time of the tube. This spread thus limits the accuracy of time measurements carried out with the system.

It follows that no study of the photomultiplier can be complete without consideration of the statistical fluctuations encountered at various stages of the transformation undergone by the incident light signal and the amplification of the resulting electric signal. These fluctuations form the main topic of the next two chapters.

3 Amplitude Fluctuations in a Photomultiplier

An experimental study of the signal fluctuations in a photomultiplier *cannot* be based on separate measurement of basic parameters depending on one another such as:
- the quantum efficiency of the photocathode;
- the collection efficiency of the input optics;
- the secondary emission coefficiency of the dynodes;
- the collection efficiency of the various stages of the multiplier.

But the factors which can be studied experimentally, independently of one another, are:
- the quantum efficiency of the photocathode,
- the overall collection efficiency of the photomultiplier,
- the statistical behaviour of the multiplier as a whole.

In order to study, the statistical properties of the multiplier, we illuminate the photomultiplier at a very low level, so that the photoelectrons reach the multiplier one by one, at intervals of time which appreciably exceed the resolving time of the associated electronic circuitry. This allows us to determine the probability distribution of the numbers of electrons received at the anode of the photomultiplier when a *single electron* enters the multiplier. This distribution, which is known as the "single-electron spectrum" characterizes the statistical properties of the multiplier.

The overall collection efficiency of the photomultiplier is also a quantity which is accessible to experiment, *if we consider it as equal to the ratio of the number of pulses counted at the anode to the number of electrons leaving the photocathode.* This method of evaluation allows the total losses of the photomultiplier to be taken into account; the actual value of these losses is not known, but is probably low (a few per cent).

The quantum efficiency can be measured quite accurately by spectrophotometric methods.

3.1 Quantum Efficiency of the Photocathode

Workers in this field have long been avware, on the basis of experimental

studies, of the importance of the quantum efficiency of the photocathode. Photoelectric emission is one of the statistical processes occurring in the the photomultiplier. If $\bar{\eta}_q$ is the mean quantum efficiency of the photocathode, it can be shown (equation 8, p. 97) that the variance of the number of electrons emitted, with a constant luminous flux falling on the cathode, is:

$$\sigma^2 = N_p \bar{\eta}_q (1 - \bar{\eta}_q) ,$$

where N_p is the number of photons striking the cathode, and $N_p \bar{\eta}_q$ is the mean number of photoelectrons emitted.

The relative variance in this case is:

$$v = \frac{1 - \bar{\eta}_q}{N_p \bar{\eta}_q} .$$

This relation shows that the value of $\bar{\eta}_q$ should be made as high as possible if we want to minimize the statistical fluctuations in the photoelectric emission. It will also be seen that the number of photons striking the photocathode should be made as high as possible, which means that the transmittance of the input window should be as high as possible.

Considerable progress has been made in increasing the sensitivity of photosensitive layers during the past decade. The T-type photocathode (Sb–Na–K–Cs), deposited on a window of B 40 glass, is the most sensitive at present for applications covering the whole of the visible spectrum. This photocathode has maximum sensitivity (65 mA/W) at 420 nm; this corresponds to a quantum efficiency of about 20%. The T-type photocathode is very useful because of its high signal-to-noise ratio (see Chapter 7). The type-C photocathode (Ag–O–Cs), which is less sensitive than the above, has the advantage of good sensitivity up to a limiting value of 1100 nm, with a maximum at about 800 nm. It is particularly suitable for the detection of radiation in the red and the near infrared regions.

Recent progress made on the type-A photocathode (Sb–Cs–O), which is used in most fast photomultipliers, has made it possible to increase its quantum efficiency to a level equivalent to that of the type-T photocathode, at least in the blue region.

However, the most progress has been made with the type-D photocathode (Sb–K–Cs), which now has a quantum efficiency of more than 20% at 400 nm. This type has a higher photoelectric threshold and a lower dark current than those mentioned above.

Type-D photocathodes are used in photomultipliers of the 56 DVP family; they allow signals as low as a single photon to be detected.

Caesium-antimonide (Sb–Cs–O) photocathodes, which so far have been deposited almost exclusively on windows of glass or fused quartz, can now be deposited on new supports such as sapphire, calcium fluoride and lithium fluoride (see Fig. 3.1). These new techniques make it possible to improve the sensitivity of photomultipliers towards the ultraviolet end of the spectrum more and more.

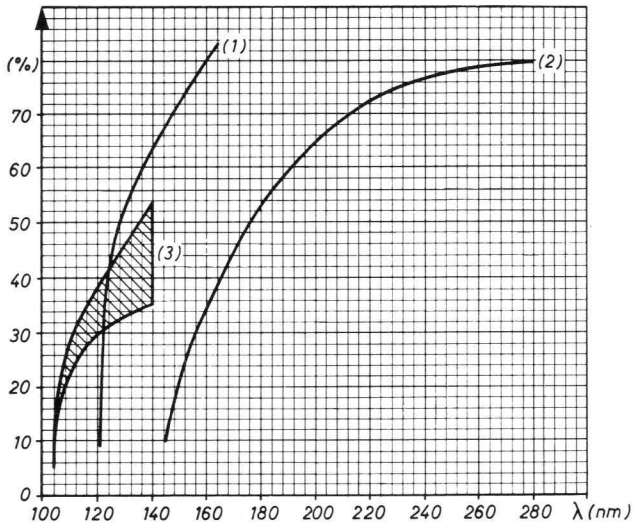

Fig. 3.1. The transmission factor as a function of the wavelength for various input windows (window thickness 1 mm).

Curve 1: fluorine
Curve 2: sapphire
Curve 3: lithium fluoride

3.2 Overall Collection Efficiency

It can easily be shown that the amplitude fluctuations which limit the performance of photomultipliers in certain respects, particularly energy resolution, depends not only on the efficiency of the conversion of information at various levels (photocathode, first dynodes) where the

number of photons or electrons involved is low, but also on the homogeneity of these efficiencies over the useful surface of the photocathodes or the dynodes. Not only should the quantum efficiency of the photocathode and the secondary emission coefficients of the first dynodes be high and homogeneous, but also the collection of electrons in the input optics and the first few stages of the multiplier should be equally homogeneous, and as close to 100% as possible.

If we choose the experimental conditions so that each photoelectron is emitted separately (single electron), we can define the overall collection efficiency η_c of the photomultiplier as the ratio of the number of anode pulses to the number of electrons leaving the photocathode.

This definition takes into account the overall losses in the first few stages of the multiplier, due the non-emission or non-collection of electrons in these dynodes in the avalanche resulting from a single electron.

Now let $\overline{N}_e$ be the number of single photoelectrons emitted per unit time, and $\overline{N}_s$ the corresponding number of signal pulses at the anode. The efficiency defined above can then be written:

$$\eta_c = \eta_{c0}(1-\alpha) = \frac{\overline{N}_s}{\overline{N}_e},$$

where η_{c0} is the collection efficiency between the photocathode and the first dynode and α is the total loss rate in the multiplier.

On the other hand, the anode sensitivity N_{ar} (measured in amperes per watt), which represents the anode current density obtained with a certain uniform irradiation of the photocathode, can also be taken as an approximate measure of the overall collection efficiency of the photomultiplier. The anode current density reflects not only the collection efficiency of the input optics η_{c0}, but also the inter-dynode collection efficiencies in the multiplier, viz:

$$\frac{I_a}{I_k} = \eta_{c0}\eta_{c1}\eta_{c2} \ldots \eta_{cn}(1-\alpha)\overline{G},$$

where $\overline{G}$ is the mean gain of the photomultiplier without collection losses. This identity between the collection efficiency and the anode sensitivity is of practical importance when we are looking for the operating conditions giving maximum collection efficiency, since it is easier to find the maximum anode current than to find the maximum collection by direct measurement.

Various methods can be used to evaluate the collection efficiency of a photomultiplier. One relatively simple method is to illuminate the cathode of the photomultiplier with light of a well-defined wavelength (obtained with the aid of a monochromator, or interference filters) and of an intensity high enough to allow sufficiently accurate measurements of the photoelectric current I_k (which is of the order of 10^{-11} A in practice). A neutral filter of known, adequate attenuation is now placed in the light beam, so that a counter attached to the anode of the photomultiplier can separate the pulses produced by the photoelectrons emitted. The number $\overline{N}_s$ of anode pulses is determined by subtracting the dark count rate (obtained with the photomultiplier unilluminated) from the total count rate observed. However, if this calculation is to be meaningful, the dark pulse rate must be sufficiently low (less than 10^4 Hz) and stable. The collection efficiency is now given by the relation:

$$\eta_c = \frac{\overline{N}_s \cdot e}{T \cdot I_k}$$

where T is the total transmittance of the neutral filters in the light beam, and e is the absolute value of the charge on the electron.

Another method, which is more difficult to put into execution, makes use of coincidence techniques (resolving time of 25 ns) together with a spark generator. This method allows the dark pulses (see Section 3.4) to be eliminated, so that only the useful anode pulses are counted. The pulses emitted by the spark generator are simultaneously sent to a reference photomultiplier by a second light path, which is equivalent to the photomultiplier under study (Fig. 3.2). The detection efficiencies of the photomultipliers under study are then compared with the aid of the reference photomultiplier. With the aid of optical filters placed in the light path, the photoemission of the photomultipliers under examination are adjusted to the same mean value of photoemission as the reference photomultipliers by means of a standard incandescent lamp, which has a much higher mean luminous intensity than the spark generator, and which can be moved into the position normally occupied by the latter.

Using one or the other of these methods, the overall collection efficiency has been measured at 420 nm for a number of photomultipliers taken from series production and for a number of specially selected reference tubes.

It may be seen from the results of these measurements (Fig. 3.3) that the collection efficiency is generally improved when the photocathode is

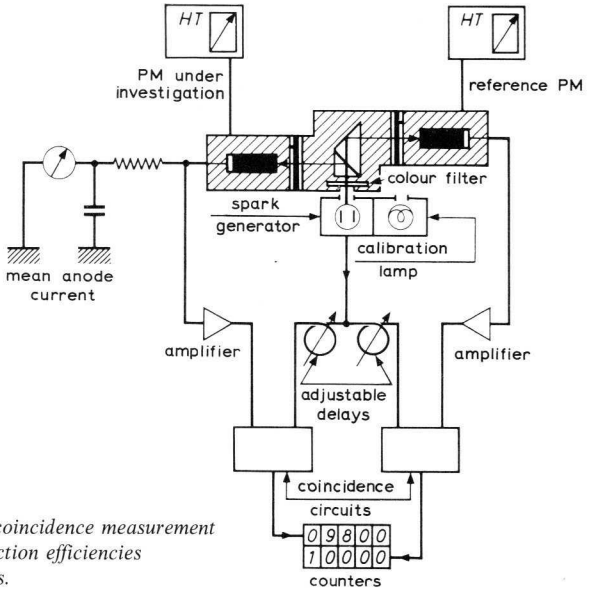

Fig. 3.2. Principle of the coincidence measurement used to compare the collection efficiencies of various photomultipliers.

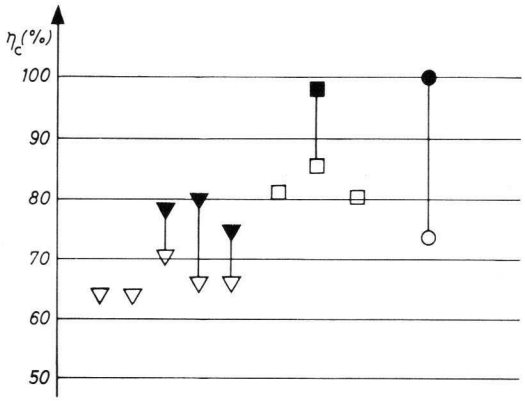

Fig. 3.3. Collection efficiencies (η_c) measured on various photomultipliers of type 56 AVP (old models) and XP 1020.

- ▽ *56 AVP, overall illumination*
- ▼ *56 AVP, illuminated in central (2 cm²)*
- □ *XP 1020, overall illumination*
- ■ *XP 1020, illuminated in central (2 cm²)*
- ○ *reference photomultiplier, overall illumination*
- ● *reference photomultiplier, illuminated in central (2 cm²)*

only illuminated in a central zone measuring a few square centimetres, where the collection is more complete. This is particulary true of the reference tube, whose collection efficiency has been estimated as nearly 100% for a circle 16 mm in diameter on the photocathode, while the corresponding value for illumination of the whole photocathode is only 75%.

A study of the variation of the collection efficiency with the wavelength of the incident light has shown (Fig. 3.4) that this efficiency increases steadily as the photon energy approaches the photoelectric threshold.

However, the main result of the measurements has been to show the decisive influence of the potentials applied to the focusing electrodes and the dynodes in the transition zone, and of the geometry of these electrodes.

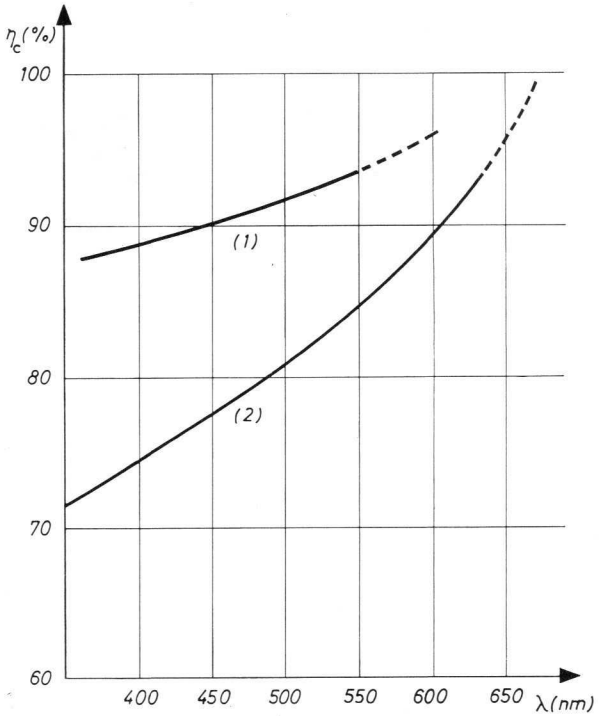

Fig. 3.4. Effect of the wavelength of the incident light on the collection efficiency η_c of photomultipliers of the types (Curve 1) XP 1020 and 56 AVP (new model) (Curve 2) 56 AVP (old model).

Let us consider the case of photomultipliers of the 56 AVP series, the input optics and multiplier transition zone of which are shown in Fig. 3.5. These tubes have two control electrodes: the focusing electrode g1 in the input optics and the second dynode S2 for the transition zone. The adjustment of the potential of g1 is critical: the electrons emitted by all points of the photocathode are only collected at a certain well defined value of this potential, the marginal electrons cannot leave the photocathode (being "blocked" by the electric field), or if they do leave this electrode they are not usefully collected and focused on the first dynode of the multiplier.

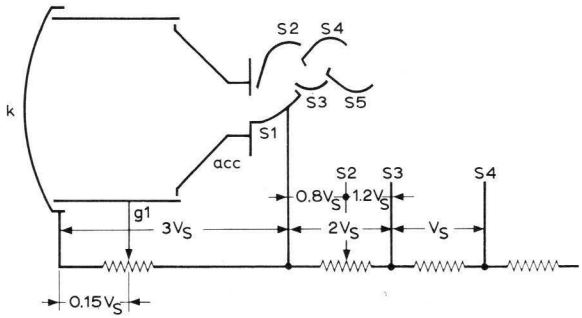

Fig. 3.5. Input optics and transition zone of the 56 AVP photomultiplier.

The form of the dynodes determines the optimum electric field used to guide the electrons from dynode to dynode, but only a part of their surface contributes to the electric current by secondary emission. It follows that electrons emitted by a point outside this useful zone do not reach the useful zone of the next dynode. The influence of the second dynode S2 on the collection efficiency is due to its position very near the first dynode.

In older models[1] of the photomultipliers types 56 AVP and 58 AVP, a special electrode g2 was provided to correct for any errors in mounting of the electrodes of the input optics and the transition zone of the multiplier. This electrode is not found in the present models of these types.

[1] Before No. 24310, as far as type 56 AVP is concerned.

Fig. 3.6 shows the relative collection efficiency η_c and the relative anode sensitivity N_a of a 56 AVP photomultiplier as functions of the potential of the focusing electrode g1. With optimum adjustement of the potentials of g1 and S2 illumination of the entire photocathode, photomultipliers of the 56 AVP type can give a collection efficiency between 80 and 85% at 240 nm (as compared with only 65 to 75% for the old models, prior to serial No. 24310).

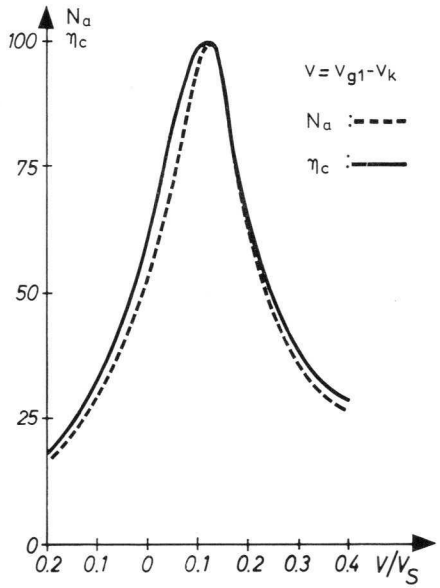

Fig. 3.6. Influence of the potential of the focusing electrode on the anode sensitivity N_a and the collection efficiency η_c of a photomultiplier of type 56 AVP. The curves were determined with overall illumination of the photocathode and are relative values.

The importance of the focusing of the electrons in the input optics and the transition zone of the multiplier has naturally led to research into the optimum form of the focusing and coupling electrodes. The modifications in the electrodes arrived at in this way has led to the development of the XP 1020-series of photomultipliers. The input optics of these tubes are quite different from those of the 56 AVP tubes (see Fig. 3.7).

The XP 1020 tubes also have two control electrodes, the focusing electrode g1 and the second dynode S2. Figures 3.8 and 3.9 show the influence

of the potentials of these electrodes on the anode sensitivity N_a and the collection efficiency η_c.

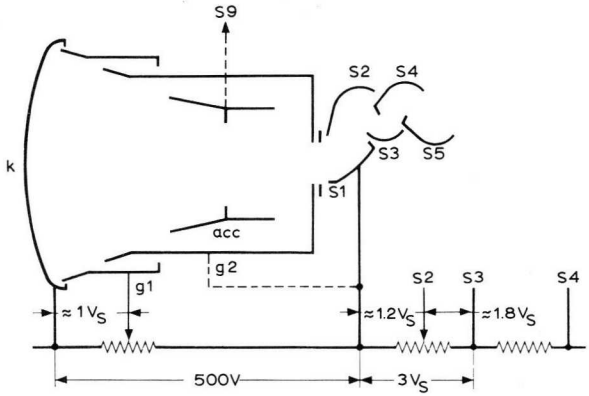

Fig. 3.7. Input optics and transition zone of the XP 1020 photomultiplier.

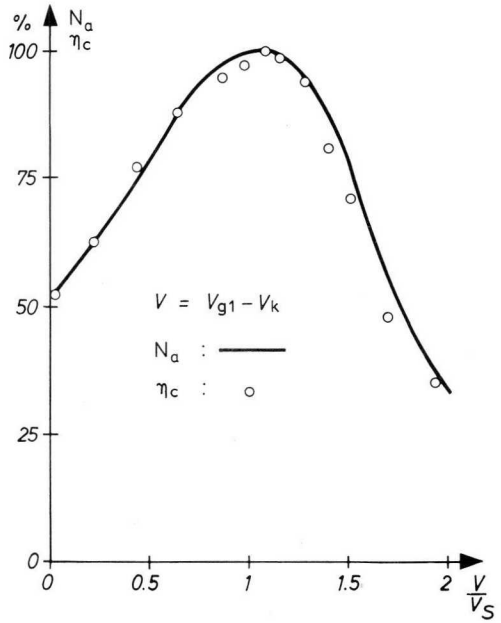

Fig. 3.8. Influence of the potential of the focusing electrode on the anode sensitivity N_a and the collection efficiency η_c of a photomultiplier of type XP 1020. Only relative values are shown.

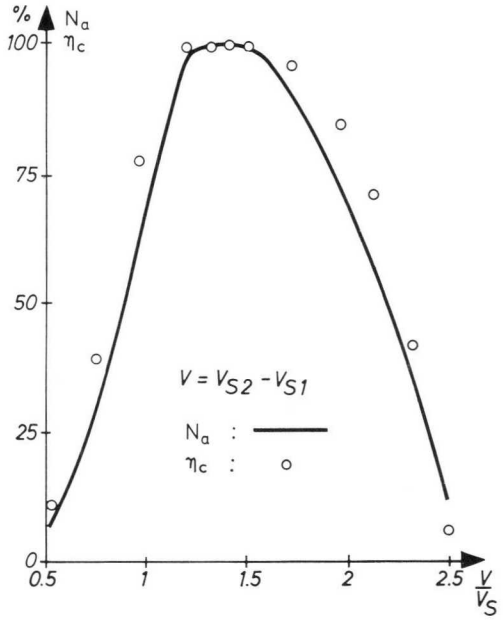

Fig. 3.9. Influence of the potential of the second dynode on the anode sensitivity N_a and the collection efficiency η_c of a photomultiplier of type XP 1020. The curve shows relative values only.

3.3 Statistical Behaviour of the Multiplier

The only way we can characterize the behaviour of the multiplier is by study of the form of the anode pulse produced when a single electron enters the multiplier. In this way, we eliminate all contributions of the photocathode and the input optics to fluctuations of the output pulse.

On the other hand, it can be shown that the relative variance of the amplitude of the anode pulse, and hence of the multiplier gain, is inversely proportional to the number of electrons entering the multiplier. The highest relative variance is thus obtained in experiments with a single incident electron.

A study of statistical properties of the multiplier based on determination of the probability distribution of the amplitude of the anode pulses in single-electron experiments will thus allow us to make deductions about the statistical fluctuations in the gain of the multiplier.

3.3.1 The Single-electron Spectrum

When an electron enters the multiplier, it gives an anode pulse whose form depends on two random variables which can be considered to be independent:

- the multiplier gain, determined by the secondary emission coefficients of the dynodes and the inter-stage collection efficiency;
- the duration of the pulse, due to the spread in the transit times of the electrons in the multiplier.

The spread in transit times of the electrons influences the width of the pulse (though it is not equal to the latter), and thus affects the signal amplitude. Under these conditions, only the integrated amplitude of the anode pulse is proportional to the total quantity of charge in the pulse, and hence to the gain of the multiplier in response to a single incident electron.

Integration of the anode pulse thus gives a pulse of well defined form, the amplitude V of which is directly proportional to the gain. Determination of the number of pulses in each amplitude interval (from V_i to $V_i+\Delta V$) in the time interval Δt thus gives the required probability distribution, known as the "single-electron spectrum", which can be written as the function $\mathrm{d}N_s/\mathrm{d}V=f(V)$.

The centre of gravity of the area under the curve defines the mean gain $\bar{G}$ of the multiplier under experimental conditions (Fig. 3.10).

The form of the distribution obtained can vary considerably, depending on the operating conditions of the photomultiplier. In order to make

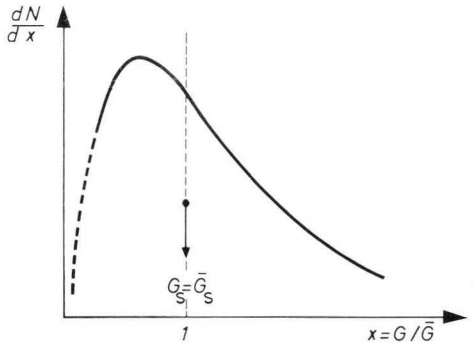

Fig. 3.10. Definition of the mean gain $\bar{G}_s$ of a multiplier system in a single electron spectrum.

various distributions comparable, they are normalized so as to correspond to the same integral number of pulses (same area under the curve) and the same mean gain of unity. This means that the spectrum is plotted as a function of the reduced gain $G/\overline{G}$ and eliminates the inevitable variations in amplification from one experiment to another.

When the photocathode is not illuminated at all, a number of pulses (whose amplitudes are distributed at random) may still be counted at the anode of the photomultiplier; the mean amplitude of these pulses represents part of the dark current (see Section 3.4). This current varies in time, and is a function not only of the temperature and the voltages applied to the photomultiplier, but also of the history of operation or storage of the tube.

The single-electron spectrum must thus be corrected for the dark current in each amplitude interval separately.

Experimental Methods and Conditions for Obtaining a Single-electron Spectrum

An electron entering the multiplier will give rise to a certain amount of charge at the output. Time $\Delta\tau$ is required for the measurement of this quantity. The output pulse will only correspond to a single electron if no other electron is emitted by the photocathode during the time $\Delta\tau$.

We can conveniently illuminate the photocathode with a incandescent lamp. A narrow frequency band is selected from the emission spectrum of this lamp by placing interference filters or colour filters in the light beam. The luminous *intensity* can be attenuated with the aid of neutral filters, if required.

The light source emits a very large number N_p of photons each second; we shall call this event A. The attenuation of the luminous flux by a factor k can be designated event B (a stochastic process, like event A). The conversion of the photons into electrons is realized with a certain quantum efficiency η_q (event C); and finally, the photoelectrons have a probability η_c of reaching the multiplier (event D).

Events B, C and D thus form a chain, at each link of which there is only one alterantive. If we suppose that the emission of the N_p photons has a Poisson distribution, it follows that this emission process followed by the chain of three events, each with only one alternative, will give a Poisson distribution for the number of photoelectrons entering the multiplier.

The distribution is characterized by the mean value:

$$\overline{N}_e = \overline{N}_p k \eta_q \eta_c$$

and by the relative variance:

$$v_e = \frac{1}{\overline{N}_p k \eta_q \eta_c} .$$

The probability distribution of the number N_e of electrons entering the multiplier in time $\Delta\tau$ may thus be written:

$$P(N_e, \Delta\tau) = \frac{e^{-\overline{N}_e \Delta\tau} (\overline{N}_e \Delta\tau)^{N_e}}{N_e!} .$$

The proportion of the output signal caused by more than one electron is given by:

$$\frac{P(N_e > 1, \Delta\tau)}{P(N_e = 1, \Delta\tau)} = \frac{1 - P(0, \Delta\tau) - P(1, \Delta\tau)}{P(1, \Delta\tau)}$$

$$= \frac{1 - e^{-\overline{N}_e \Delta\tau}(1 + \overline{N}_e \Delta\tau)}{\overline{N}_e \Delta\tau e^{-\overline{N}_e \Delta\tau}} \approx \frac{\overline{N}_e \Delta\tau}{2}$$

if

$$\overline{N}_e \Delta\tau \ll 1 .$$

Now we are able to calculate the extent to which the luminous flux should be attenuated in order to ensure that as many anode pulses as possible are produced due to a single electron entering the multiplier.

Two methods can be used to give single-electron spectra. The first method (see Fig. 3.11) makes use of a continuous light source such as an incandescent lamp. We now determine the spectrum of the dark pulses (see Section 3.4), and the spectrum of the pulses produced by the photomultiplier when it is illuminated at a very low level by the light source. The difference between these two spectra is the single electron spectrum. However, this method is only applicable to photomultipliers with a sufficiently low cathode dark current (less than about 10^{-16} A/cm^2. Having regard to the time available for the analysis of a pulse in the electronic equipment (generally of the order of 10 to 20 μs), it will be clear that the photoelectric current when the light source is on will often not be larger than the dark current.

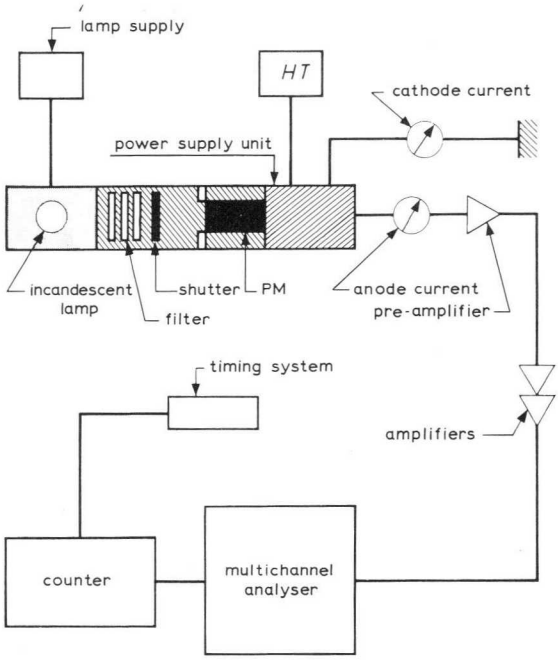

Fig. 3.11. Principle of determination of single-electron spectrum with a continuous light source.

The second method (see Fig. 3.12) uses a source of pulses of light with a duration of some nanoseconds and a repetition frequency of the order of 5 to 10 kHz. This gives a synchronous electrical pulse which can be used to open the gate of a multichannel spectrum analyser. A large part of the dark pulses will thus be eliminated in a simple way. A few noise pulses will still get through the gate, but the subtraction of the two spectra will be carried out under much more favourable circumstances than in the preceding method. Unfortunately, this second method is very time-consuming, since the light still has to be attenuated to such an extent that the probability of counting more than one photoelectron per pulse is negligible; this means that in general only a very small proportion of the light pulses reaching the photocathode will actually give rise to a photoelectron.

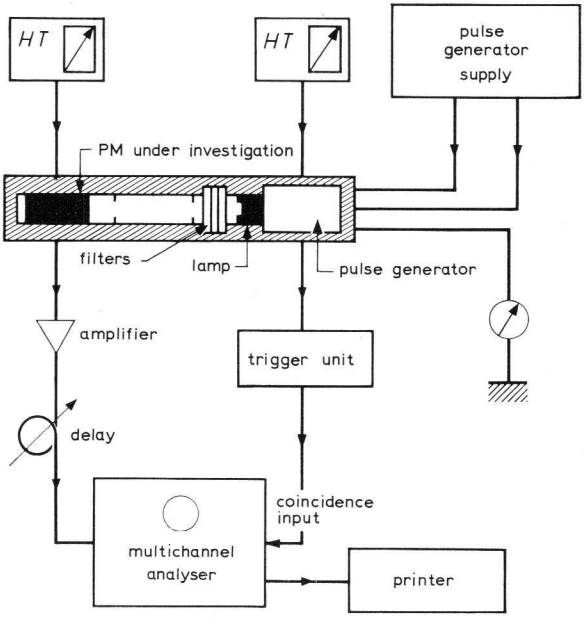

Fig. 3.12. Principle of determination of single-electron spectrum with a pulsed light source and a coincidence technique.

Calculation of the Relative Variance of the Gain

Determination of the single-electron spectrum under the experimental conditions described above allows us, as we have seen, to evaluate the fluctuations of the gain, and hence to calculate the relative variance of the gain, v_G.

This quantity can be calculated from a number of experimental points (one per channel), making use of the definitions of σ^2 and v given in the list of symbols at the front of the book.

However, we know that when an electron enters the multiplier, there is a probability $P(\alpha)$ that no bunch of electrons will arrive at the anode (see Section 3.2), and in certain cases α may be far from negligible.

The relative variance of the gain derived from the single-electron striking spectrum we may denote by v_s, will thus be less than the real value v_G of this variance.

Under the conditions described above, it is possible to correct for the error due to the total losses in the multiplier. For this purpose, let us define the overall collection efficiency of the multiplier (η'_c) as the ratio of the number of anode pulses to the corresponding number of electrons striking the first dynode[1], so that:

$$\eta'_c = 1 - \alpha .$$

The amplification process can thus be considered as equivalent to the combination of two events in cascade: the collection of the electrons (with certain loss), and the multiplication of these electrons without any further losses.

Since the collection is a stochastic process, its relative variance may be written (see Appendix 1, equations 3 and 4):

$$\frac{1-\eta'_c}{\bar{\eta}'_c}$$

It now follows (see equations 10 and 11 of Appendix 1, relating to a series of events in cascade) that the real mean gain $\bar{G}_r$ can be expressed as:

$$\bar{G}_r = \bar{\eta}'_c \bar{G}_s$$

and the relative variance of this gain as:

$$v_{G_r} = \frac{1-\eta'_c}{\bar{\eta}'_c} + \frac{v_s}{\bar{\eta}'_c}$$

where $\bar{G}_s$ and v_s are the mean gain and its relative variance as calculated from the experimental single electron spectrum.

3.3.2 Mathematical Expression of Gain Fluctuations

The influence of the various basic parameters of the multiplier on the fluctuations of the gain, and the means which can be used to reduce these fluctuations, follow from the results of the mathematical discussion given in Appendix 1. We shall summarize these results briefly here.

---

[1] The quantities η_c and η'_c should not be confused. They are related by the equation $\eta_c = \eta_{co} \cdot \eta'_c$. The value of η_{co} should be made as near to unity as possible by illuminating only a small part of the photocathode.

The multiplication of electrons in the multiplier is assumed to be a stochastic process, leading (on receipt of a single electron at the input of the multiplier) to a certain distribution of electrons at the anode, characterized by:

a mean value $\bar{G}_r$ of the multiplier gain, and

a relative variance v_{G_r}.

$\bar{G}_r$ represents the true mean gain of the multiplier. Now the overall gain of the multiplier can be expressed in terms of the secondary emission coefficients δ_i of the various dynodes and the various inter-stage collection efficiencies η_{ci}, as follows:

$$\bar{G}_r = \prod_{i=1}^{n} \eta_{ci} \delta_i \tag{1}$$

where n is the total number of dynodes.

The relative variance of the multiplier can be written as follows in terms of the same parameters (see Appendix 1 equation 14):

$$v_{G_r} = v_{g1} + \frac{v_{g2}}{\eta_{c1}\delta_1} + \frac{v_{g3}}{\eta_{c1}\delta_1\eta_{c2}\delta_2} + \ldots + \frac{v_{gn}}{\eta_{c1}\delta_1\eta_{c2}\delta_2 \ldots \eta_{cn-1}\delta_{n-1}} \tag{2}$$

where v_{gi} represents the relative variance of the gain of the i^{th} stage:

$$g_i = \eta_{ci}\delta_i \; (i = 1, 2, \ldots n).$$

Now it will be clear from equation (2) that the dynodes of the transition zone play the major part in determining the relative variance of the multiplier again. This means that if we want to minimize this variance, we should choose the distribution of the gain between the stages *so that the gain per stage is highest in the transition zone.*

If we assume that the first stage of the multiplier has a gain g_1, and that all other stages have the same (lower) gain g, the overall gain of the multiplier and its variance may be represented by simplier expressions (for $n \gg 1$ and $g > 1$), viz:

$$\bar{G}_r = g_1 g^{n-1}$$

and

$$v_{G_r} = v_{g1} + \frac{v_g}{g_1} \frac{g}{(g-1)} \tag{3}$$

where v_g is the relative variance of the gain per stage.

Assuming that the secondary electrons emitted by the dynodes have a Poisson distribution, we find that the relative variance of the gain per stage is equal to $1/g$. In this case, equation (3) may be written in the form:

$$v_{G_r} \simeq \frac{1}{g_1} \frac{g}{g-1} \tag{4}$$

3.3.3 Influence of Secondary Emission Coefficients and Collection Efficiency on the Single-electron Spectrum

Equation (4), which is based on the assumption that the secondary emission has a Poisson distribution, shows that increasing the secondary emission coefficient of the first dynode is very effective in reducing the relative variance of the electron distribution at the anode. For this reason, photomultipliers like the XP 1020, for example, have been designed for a voltage of 500 V between the cathode and the first dynode under normal operation conditions (see Fig. 3.7).

However, while equation (2) shows that the first stage of the multiplier is mainly responsible for the fluctuations in the anode pulses due to the random nature of the secondary emission process, the stages which follow also contribute to this fluctuation. Under conditions which render the coupling between successive stages close to unity (collection efficiency 100%), an increase in the secondary emission coefficient of the dynodes in the transition zone will act in the same sense as the increase in the first stage, and will thus also help to reduce the variance of the single-electron spectrum. In general, therefore, it is thus advisable *to make the supply voltages of the dynodes of the transition zone decrease gradually.* This will not have an adverse effect on the focusing properties of the multiplier as a whole, but will have the effect of increasing the secondary emission coefficients of these dynodes. Fig. 3.13 shows how the single-electron spectrum varies when the potentials of the first few dynodes of a photomultiplier are varied.

Similarly, equation (2) shows the importance of the collection efficiency of the various stages of the multiplier–particulary the first ones, since it is here that the main electron losses are produced.

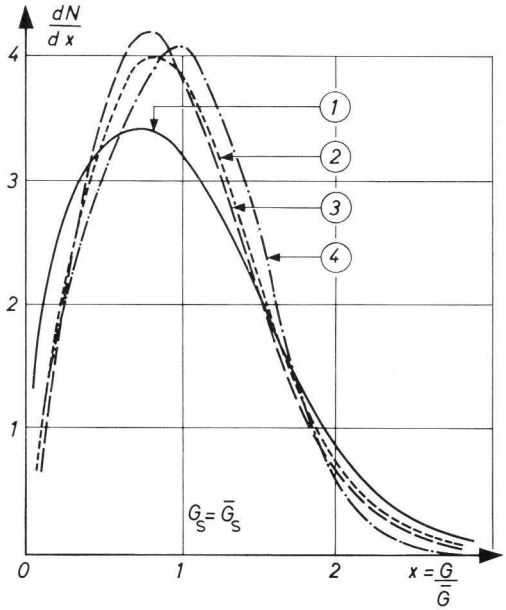

Fig. 3.13. Influence of the distribution of the potential between the first few stages of a photomultiplier on the single-electron spectrum.

Voltage distributions and corresponding relative variance of single-electron spectrum:

voltage between electrodes	curve 1	curve 2	curve 3	curve 4
k and S1	1.2 V_s	3 V_s	5 V_s	4 V_s
S1 and S2	1 V_s	1 V_s	1 V_s	2.8 V_s
S2 and S3	1.1 V_s	1.1 V_s	1.1 V_s	2.4 V_s
S3 and S4	0.9 V_s	0.9 V_s	0.9 V_s	1 V_s
S4 and S5	1 V_s	1 V_s	1 V_s	1 V_s
relative variance v_m	0.37	0.28	0.26	0.23

3.4 Dark Current Noise Pulses

In the absence of all light incident on the photocathode, a number of weak pulses will still be observed at the anode of the photomultiplier; the distribution of these pulses in amplitude and in time is completely random. The mean amplitude of these current pulses represents part of the anode dark current. In this book, we shall simply refer to these pulses as *dark pulses.*

These dark pulses are a particular nuisance when the level of the useful signal to be detected is low, as is the case of soft X-rays, low-energy beta radiation (like that from tritium or carbon-14), or high-energy particles which only produce a few photons per pulse (by the Cerenkov effect).

The amplitude distribution of the dark pulses thus forms a limit to the detection of phenomena which only produce a very small number of electrons at the photocathode. Disregarding the noise of the photomultiplier, the detection limit will be reached when the phenomenon under study only gives rise to one photoelectron per pulse at the cathode.

Dark pulses may be divided into two classes, depending on their source. One part of the dark pulses is produced in the input optics. These pulses have high or medium relative amplitudes, and since they come from individual electrons above the multiplier their distribution is that of the single-electron spectrum.

The second part consists of pulses of low relative amplitude; these pulses are generally much more in number. It will be clear, therefore, that they arise in the multiplier.

The cause of the dark pulses is difficult to define with certainty. Many of them are doubtless due the thermionic or field-effect emission from the photocathode and the other electrodes. However, there are a number of other causes which may be cited, in particular the bombardment of the photocathode by ions from the residual gas, emission from the photocathode under the influence of scintillations in the glass envelope of the tube produced by radioactive nuclei in the glass (potassium-40) or by bombardment with electrons, luminescence in the later stages of the multiplier, and breakdowns between the electrodes.

Fig. 3.14 shows the noise spectrum of a 56 DVP photomultiplier provided with the type-D photocathode. The right-hand part of this curve represents the distribution of the pulses produced by single electrons from the photocathode, while on the left we see the curve corresponding to the high-density, low-energy pulses from the multiplier.

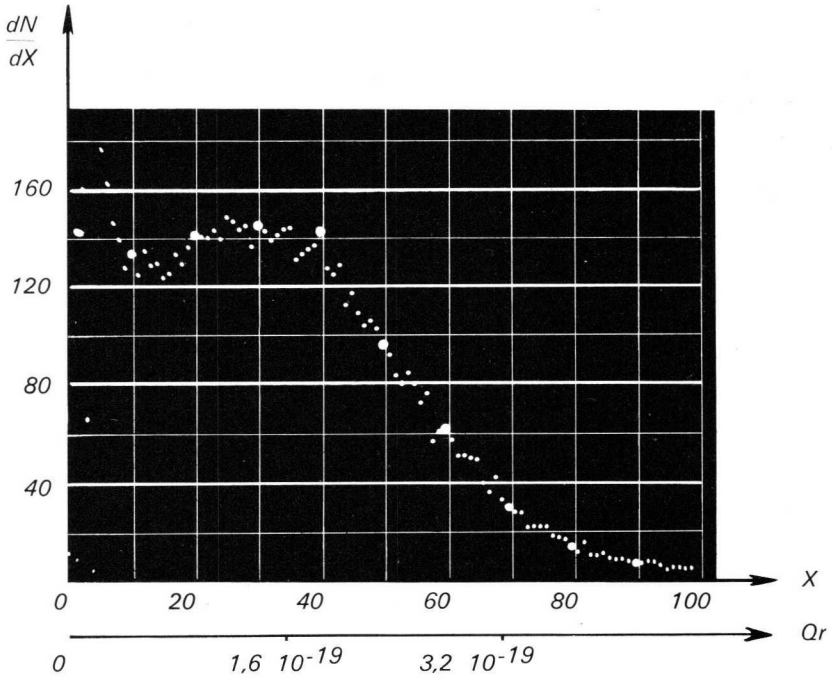

Fig. 3.14. Noise spectrum of a 56 DVP photomultiplier.
Ordinate: dN/dX = counting density in pulse per minute per channel;
Abscissa: X = number of channel.
Q_r = *reduced charge per pulse* $= \dfrac{\text{charge per pulse}}{\bar{G}}$

3.5 Energy Resolution

When a scintillation counter is used for the measurement of the energy of a particle or electromagnetic radiation, the most important characteristic of the counter is its resolution, i.e. its ability to separate two radiations of neighbouring energies.

The charge Q collected at the output of the scintillation counter (the anode of the photomultiplier) is proportional to the energy of the incident radiation. However, we have seen that the number of elementary charges

arriving at the anode is subject to random fluctuations due to the stochastic nature of the various conversion processes undergone by the electric signal. With a monoenergetic radiation of energy W_0 we would get a constant charge Q_0 at the anode if the detector were completely free of sources of fluctuation; the energy spectrum, corresponding to the amplitude distribution of the pulses, would then consist of *a single line of energy* W_0. However, since random fluctuations do occur. both in the scintillator and in the photomultiplier, the line will have a certain width, as indicated in Fig. 3.15.

This width of the spectral lines makes it difficult for two radiations whose energies are very close together to be separated. Before the two lines can be distinguished they must be separated by an energy distance of at least ΔW (see Fig. 3.15). This leads us to define the resolution of a scintillation counter by the ratio:

$$R = \frac{\Delta W}{W_0}.$$

This is a dimensionless number which is generally expressed as a percentage. The resolution varies with the energy of the incident radiation and, of course, depends on the intrinsic statistical properties of the scintillation counter.

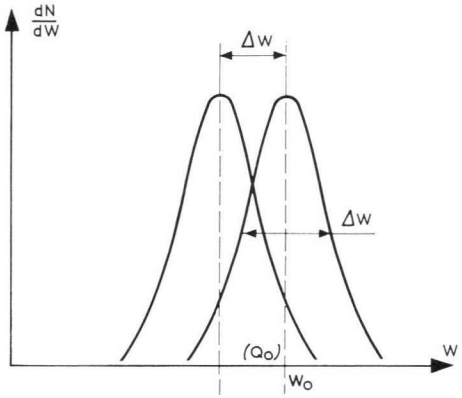

Fig. 3.15. Definition of energy resolution.

In calculating this expression it can be assumed that if the number of photons striking the photocathode due to scintillation is high, the amplitude distribution of the pulses at the output of the photomultiplier is little different from a Gaussian distribution. Consequently, the peak value, relative to the mean height of the spectral curve, is given by the expression:

$$\frac{\Delta W}{W_0} = 2.36\,(\upsilon_Q)^{\frac{1}{2}}$$

where υ_Q represents the relative variance of the electron distribution at the output of the photomultiplier. Using the same value of υ_Q, derived from Appendix 2, equation (18), the expression for the resolving power, in terms of the parameters of the scintillator, can be expressed in the form:

$$R = 2.36\left(\upsilon_N + \frac{1-\eta_c\eta_q+\upsilon_s}{\overline{N}_p\eta_c\eta_q}\right)^{\frac{1}{2}} \tag{5}$$

where $\overline{N}_p$ is the mean number of photons striking the photocathode at each scintillation, and υ_N is the relative variance of this number.

These quantities are not therefore directly concerned with the behaviour of the photomultiplier, but are dependent upon the type of scintillator with which the photomultiplier is used, and on the optical coupling between the scintillator and the input window of the photomultiplier.

The other quantities η_q and η_c, are the quantum efficiency and overall collection efficiency of the photomultiplier. Equation (5) thus confirms the need for obtaining maximum quantum yield and collection efficiency. The term υ_s represents the multiplier system; it is the relative variance of a single-electron spectrum (see Section 3.3.1).

The spectrometric characteristics of a photomultiplier are taken in association with a NaI (T1) scintillator. The resolving power is measured by means of 662 keV gamma radiation of caesium 137.

At the present time, the highest energy resolving power that can be obtained is in the neighbourhood of 7 %, whereas other forms of detector have resolutions of 9 %, this value varying slightly from one detector to another.

4 Time Fluctuations in a Photomultiplier

4.1 Speed of Response

When a photomultiplier receives luminous information at its photocathode, a very short period of time elapses between the moment that the electrical pulse is received at the anode. This time is related to the time taken for the electron avalanche to pass through the tube, and it depends on the voltage distribution between the various stages of the photomultiplier. In other words, there is a certain delay between the production of the luminous phenomenon in question and its detection. However, this delay only matters when the electrical signal from the photomultiplier has to be synchronized with the observed light source (e.g. for triggering a camera).

On the other hand, this delay time is subject to random fluctuations due to the random differences in the transit time of electrons between two electrodes, and these flucuations become very important when the photomultiplier is used for the measurement of very short intervals of time (e.g. less than a nanosecond).

The spread in the transit times of the electrons also has another consequence; it widens the response function of the photomultiplier to a very short light pulse, thus introducing a limitation on the observation of very rapid variations of the luminous intensity.

The term "speed of response" can thus have a number of different meanings when applied to photomultipliers, corresponding to quite distinct characteristics of these tubes:

- if the electrical pulse has to be synchronized with the luminous phenomenon under investigation, it is the overall transit time of the bunch of electrons through the tube which characterizes its speed;
- if the photomultiplier is used for the precise measurement of short intervals of time between two pulses (the time being measured from the passage of an arbitrarily chosen characteristic point such as the centre of gravity of the pulse, the point of maximum amplitude, 50 % of rise time, etc.), then the speed of the tube is characterized by the maximum variation in the overall transit time of the bunch of electrons through the tube–in other words by the uncertainty about the exact moment at which the anode pulse will occur (Fig. 4.1);

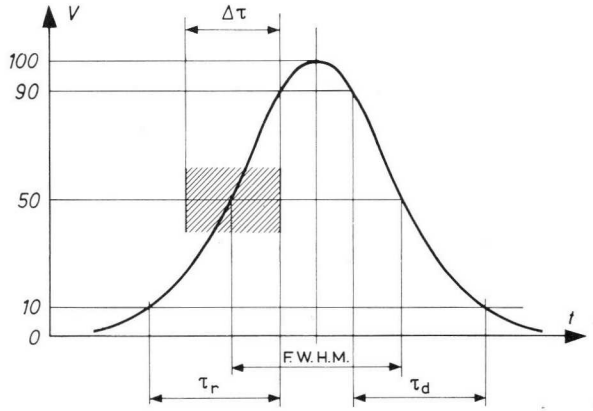

Fig. 4.1. Characteristics of the anode pulse of a photomultiplier.
F.W.H.M.: full width half maximum
$\Delta\tau$: overall transit-time spread.
τ_r: rise time
τ_d: fall time

– the most usual meaning of the "speed" of a photomultiplier is its ability to separate pulses occurring very close together in time, i.e. its temperoal resolving power.

The resolving power of a photomultiplier will be higher as the anode current pulse produced in response to a very brief light pulse is shorter. An ideal photomultiplier would thus give an anode current pulse in the form of a δ Dirac pulse when stimulated by a light pulse of the same form. In fact, as we shall see, the pulse transmitted by the photomultiplier is broadened; the rise time and the half-height width of the pulse response are thus the best measures of the speed of the tube in this sense.

The distinction between these last two definitions is very important, even though the measures which reduce the fluctuations in transit time are, in principle, precisly the same as those which improve the resolving power. However, we shall see that those measures do not apply equally to all stages of the photomultiplier, and that they are more difficult to apply in the second case.

At present, a photomultiplier is said to be "fast" when it can give a current pulse the rise time and half-height width of which do not exceed a few nanoseconds, in response to a light pulse of very short duration (less than 10^{-10} s).

4.2 Effects of Statistical Fluctuations on Response Time

We shall now consider how the different parts of the photomultiplier contribute to the fluctuations which lead to changes in the response time of the tube. It should be remembered that the various parts of the tube do not all contribute in the same proportion to the variations in the overall transit time of the electron bunch, or to the broadening of the output pulse produced in response to a very brief light pulse. The mean form of the anode pulse depends on variations in the transit time of the electrons produced at all stages of the photomultiplier, including the input optics. The rise time and the width of the pulse can thus be determined by summing the variances in transit time produced by the dispersion phenomena at the various points of the tube. Since what we are doing in this case is in fact summing squares, the influence of the input optics, considered separately, on the width of the anode pulse will be almost negligible; it only represents one source of dispersion among the many (one per stage) found in the tube. On the other hand, the fluctuations in the overall transit time of the electron bunch in the tube (due, as we shall see, to the statistical variations in the gain and the spread in the transit time of the electrons) are caused almost entirely by the input optics and the first few stages of the multiplier.

In the next section we shall describe the mechanism of the fluctuations in the transit time of the electrons in the tube, due the differences between the various electron trajectories which affect the form and the delay of the response of the photomultiplier.

4.2.1 Fluctuations in the Transit Time of the Electrons

The transit time of the electrons in the tube is subject to statistical variations depending on the initial conditions of motions of the individual electrons. Two electrons, emitted simultaneously or in succession, may follow different paths between two successive electrodes, for two distinct reasons:

a. they start from different points, or
b. they start from the same point, but with different initial velocities (in magnitude and direction).

Let us consider, by way of example, two successive dynodes (Fig. 4.2), and examine the effects produced by the differences in transit time between these two electrodes.

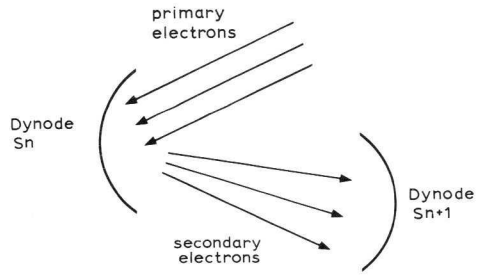

Fig. 4.2. Model for fluctuations in transit time of electrons between two successive dynodes, Sn and Sn+1.

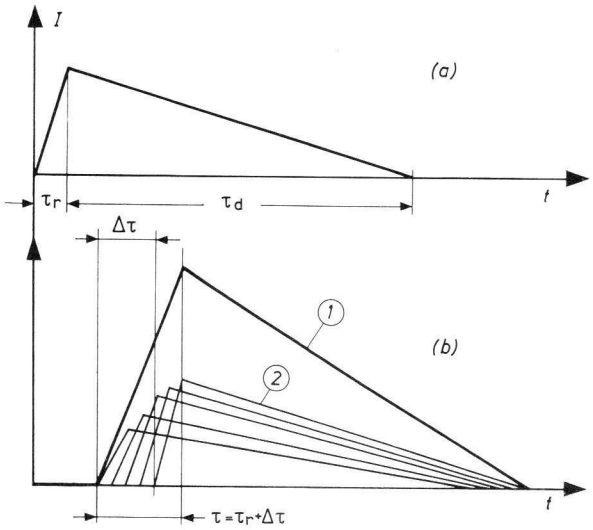

Fig. 4.3. Formation of a current pulse by summation of elementary responses shifted in time by the differences in transit time between the different zones of the photocathode or of a dynode.

Ordinate: pulse amplitude
Abscissa: time.
a. electrical pulse at dynode Sn;
τ_r *= rise time*
τ_d *= fall time*
b. electrical pulse at dynode Sn+1;
Curve 1 overall response
Curve 2 elementary non-isochronous responses

We start considering the case where the whole useful surface of the dynode Sn is excited simultaneously by a flux of primary electrons. A uniform emission of secondary electrons is provided, all of which move perpendicular to the surface of the dynode, with the same initial velocity. If all the electron trajectories between the two electrodes were strictly equivalent, the electron flux arriving at the dynode Sn + 1 would have the same distribution in time as the electrical signal transported by the incident electron flux.

However, the trajectories followed by the electrons emitted by the different parts of the dynode Sn are different. This means that the electrical signal transmitted will be distorted by the superposition of the various responses, all of which have the same form but are displaced in time with respect to one another by intervals which reflect faithfully the differences in the paths travelled by the electrons. This "non-isochronism" is illustrated in Fig. 4.3.

Let us now suppose that the arrival of a single primary electron at the dynode Sn gives rise to the production of a single secondary electron, the normal tangential components of whose initial velocity vary from one experiment to another by virtue of the stochastic nature of the secondary-emission process. This electron may thus follow a number of different paths; in this case the non-isochronism will not result in distortion of the corresponding charge pulse, but will introduce an uncertainty as to its moment of appearance. This is illustrated in Fig. 4.4.

Now the real case lies somewhere between the emission of a single electron by the dynode Sn and the simultaneous emission of a bunch of electrons by the whole surface of the dynode. It will be clear that if the various electron trajectories are not isochronous, the arrival of the secondary electrons at the dynode Sn + 1 will be spread out over a time interval Δt, equal to the difference between the longest and the shortest transit times.

This effect of the non-isochronism of the electron trajectories will be repeated at every single stage of the photomultiplier, including the input optics. The total effect produced at the anode of the photomultiplier may be found by summing the squares of the standard deviations (i.e. summing the variances) of the transit time found at the various stages.

It follows that excitation of the photocathode by a luminous signal in the form of a unit pulse will give rise at the anode to a current pulse with finite rise and fall times. The form of the leading and trailing edges of the anode pulse depends on the way in which the photoelectrons or the

secondary electrons are distributed between the various possible trajectories according to their point of emission and their initial velocity. This distribution generally varies from one pulse to another; the non-isochronism thus causes a unit pulse to be transformed into a pulse with sloping edges and, moreover, causes this signal to be variable in form and in position. This is illustrated in Fig. 4.5, which may be regarded as a generalization of Fig. 4.4.

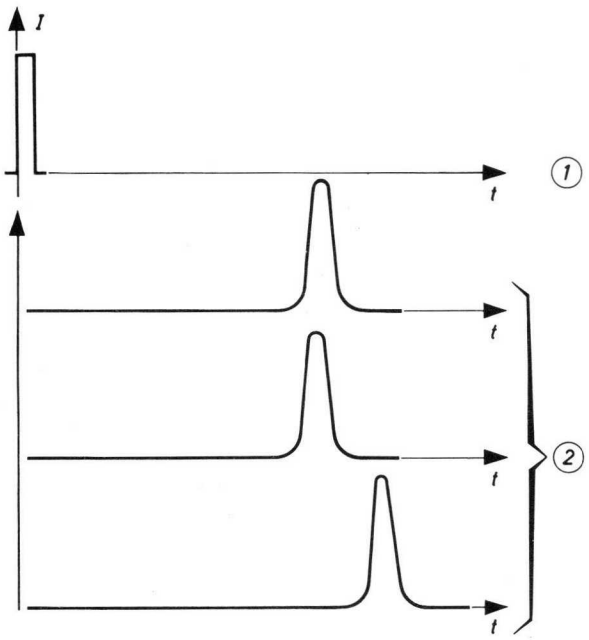

Fig. 4.4. Timing diagram of pulses received by the dynode Sn+1 when the dynode Sn only emits a single electron at a time, the transit time of which varies from one experiment to another.
1. signal corresponding to the emission of a single electron by the dynode Sn;
2. Possible instants at which the pulse can reach Sn+1.

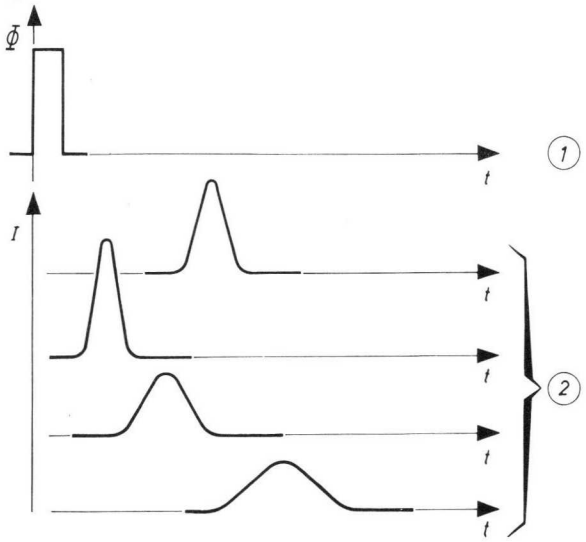

Fig. 4.5. Timing diagram of pulses obtained when the cathode emits a bunch of electrons. Under the influence of the differences in transit time, this bunch spreads out more or less, and its mean delay time fluctuates.

Ordinate: Φ = luminous flux
I = pulse current
Abscissa: time

1. Luminous signal falling on photocathode.

2. Various possible forms and times of arrival of electrical pulses at the anode of the photomultiplier.

4.2.2 Mathematical Formulation of Time Fluctuations

In this section we shall summarize certain results of a mathematical theory developed by E. Gatti (see Appendix 3), concerning time fluctuations in a photomultiplier.

Since the information received by the photocathode is itself subject to statistical variations, in order to study the distribution of the anode pulse resulting from incident photons, the emission of a single photoelectron from the photocathode is now considered.

We have seen that fluctuations in the transit time of electrons between

the electrodes and the inhomogeneity of the electrode materials lead to a broadening of the response of the photomultiplier. Further, the moment of appearance of a pulse (taken as the moment of passage of a characteristic element of the pulse, generally its centre of gravity) also exhibits random variations about a mean value from one experiment to another.

We may thus characterize, in accordance with the theory of E. Gatti (2), the anode pulse by abscissa of its centre of gravity on the time axis on the one hand, and by its width on the other hand; the pulse can thus be defined by a function $f(t, \psi, \chi)$, where ψ is a measure of the width of the anode pulse and χ is a statistical variable having time dimensions with an average value of zero and a variance σ_χ^2. This variable accounts for the device time spread and is the variance of the time interval between the instant of emission of one photoelectron and the instant at which the centre of gravity of the pulse arrives as the output.

ψ and χ are parameters which vary statistically from one photoelectron to the next. If we normalize the response function with respect to unity, we may write:

$$\int_0^\infty f(t, \psi, \chi)\, \mathrm{d}t = 1 .$$

ψ is defined as the 2nd-order moment of the function $f(t, \psi, \chi)$ by:

$$\psi^2 = \int_0^\infty (t-b)^2 f(t, \psi, \chi)\, \mathrm{d}t ,$$

where b is the abscissa of the centre of gravity of the output pulse on the time axis.

It may be proved, only taking account of the stochastic nature of the secondary-emission process (Appendix 3, equation 26), that the relative variance of ψ may be written:

$$v_\psi = \frac{1}{(g-1)n^2}\left(1 + \frac{3}{2} v_g\right), \tag{6}$$

where g is the gain per stage (supposed to be the same for all dynodes), v_g is the relative variance of this gain (normally equal to $1/g$) and n is the number of dynodes.

Similarly, the variance of χ may be written (Appendix 3, equation 30):

$$\sigma_\chi{}^2 = \sigma_{CS1}^2 + \frac{\sigma_{SS}^2}{g-1}(1+2\upsilon_g)\,, \tag{7}$$

where σ_{CS1}^2 is the variance of the transit time of the electrons between the cathode and the first dynode, and σ_{SS}^2 is the variance of the transit time between successive dynodes. These two terms are thus linked with the non-isochronism of the electron trajectories in the input optics of the photomultiplier.

The above equations have been derived on the assumption that all stages of the multiplier have the same characteristics (iterative structure). In practice, the geometry of the first two dynodes (S1 and S2) differs from that of the other dynodes. Moreover, since the first stages of the multiplier have more influence on the amplitude fluctuations of the output pulses, the gain of these dynodes is chosen higher than that of the dynodes which follow (see Section 3.2). Equation (7) should thus be modified, to read:

$$\sigma_\chi^2 = \sigma_{CS1}^2 + \frac{\sigma_{S1S2}^2}{g_1}(1+\upsilon_{g_1}) + \frac{\sigma_{SS}^2}{g_1(g-1)}(1+\upsilon_g) \tag{8}$$

where σ_{S1S2}^2 is the variance of the transit time between the first two dynodes, g_1 is the gain of the first stage and υ_{g_1} is its relative variance.

Finally, we assume that the mean value $\bar{\psi}$ of ψ (Appendix 3, equation 25) is given by:

$$\bar{\psi}^2 = n\sigma_{SS}^2\,. \tag{9}$$

Equation (9) thus shows that the width of the anode pulse, for a given structure of the multiplier, only depends on the variance of the transit time of the electrons between successive dynodes. The input optics (which we have not considered here, since we are dealing with the emission of a single photoelectron) would actually have a negligible influence on the width $\bar{\psi}$ of the pulse.

Concerning the centre of gravity of the pulse, however, equation (8) shows that the fluctuations of the moment of arrival of the output pulse depend on two factors:

- the variance of the transit time of the electrons in the input optics and between the dynodes of the multiplier;
- the variance of the gain of each stage.

Moreover, equation (8) confirms that the fluctuations in the moment of arrival of the output pulse (the fluctuations in the overall transit time) are mainly determined by the input optics and by the first couple of stages of the multiplier.

Finally, we see that in order to reduce the variance σ_χ^2 of the overall transit time and to improve the resolving power (lower value of $\bar{\psi}$), we need to reduce the standard deviations of the transit times σ_{CS1} and σ_{S1S2}, i.e. to correct for transit-time spread and transit-time difference in the input optics and in the first few stages of the multiplier as far as possible. Increasing the gain per stage within the permissible limits, especially for the first few stages, will have a similar effect.

4.3 Transit-time Spread and Transit-time Difference

We have seen that when an electron leaves an electrode (the photocathode or a dynode) for the next, it may do so from different points, or from the same point with different initial velocities, in successive experiments. Both effects can give rise to transit-time errors.

By analogy with light optics, we might call the first type of transit-time error geometric aberration and the second type chromatic aberration. However, we shall from now on use the terms *transit-time difference* and *transit-time spread.* (See Application Book "Photomultipliers" p. 17.).

In the following sections, we shall analyse the causes of the transit-time errors occurring in the various parts of the photomultiplier, and indicate the steps which could be or have been taken to improve its performance in this respect.

4.3.1 Input Optics

Causes of transit-time errors

Although transit-time spread and transit-time differences in fact occur together, it is convenient to consider them separately and to consider values for these two effects taken from the three fast photomultipliers 56 AVP, 58 AVP, XP 1020.

Transit-time difference is purely geometrical in nature. It may be defined as the difference in transit time between an electron trajectory starting from the centre of the photocathode and other trajectories starting from

other points on the surface of the cathode, it being assumed that all electrons have zero initial velocity.

Let us consider two electrons, emitted with zero initial velocity and following two different trajectories L whose lengths differ by a small amount ΔL in a uniform electric field E. It can be shown that the transit-time difference between these two trajectories may be written:

$$\Delta t \simeq \sqrt{\frac{m}{2e}} \frac{1}{\sqrt{E}} \frac{\Delta L}{\sqrt{L}} \quad \text{(in SI units)}. \tag{10}$$

With normal settings of the photomultiplier, typical values of the transit-time difference are about 5×10^{-10} s at 20 mm from the centre for a 56 AVP photomultiplier, 15×10^{-10} s at 52 mm from the centre for a 58 AVP and 2×10^{-10} s at 20 mm from the centre for an XP 1020.

These values refer to a delay of the peripheral trajectory with respect to the central trajectory. The curves of Fig. 4.6 show experimentally determined transit-time differences, measured on three tubes of type 56 AVP. The transit-time difference should theoretically show rotational symmetry; in practice however, it normally deviated from this. In fact, the inclination which the first dynode S1 must have with respect to the axis of the input optics means that all principal electron rays would have to converge on the same point of S1 to give the transit-time difference perfect rotational symmetry (see Fig. 4.7).

The slightest difference between the real and theoretical geometries can thus alter conditions appreciably in this respect. The oblique section of the electron beam by S1 thus introduces extra transit-time differences of the order of 10^{-10} s per millimetre of diameter of the focal spot produced by the main rays on S1.

A change in the voltages applied to the electrodes of the input optics from their nominal values will also affect the diameter of the focal spot, and may aggravate the above mentioned effect (but may equally well correct it, in part).

Finally, *a magnetic field* can cause deformation of the electron trajectories and alteration of the distribution of the transit times. It should be borne in mind that the magnetic field of the earth can also have this effect.

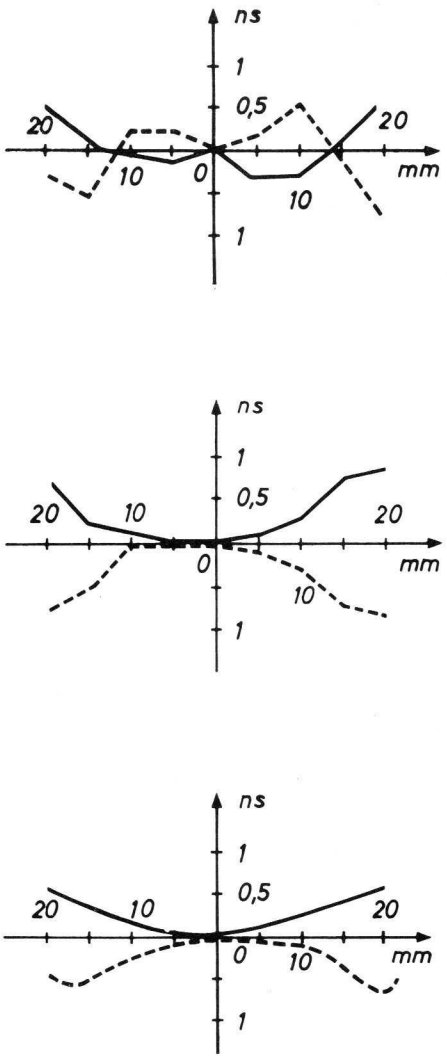

Fig. 4.6. Characteristics showing transit-time differences as a function of the point of emission considered on the cathode, for three 56 AVP tubes scanned parallel (full lines) and at right angles (broken lines) to the axes of the dynodes.

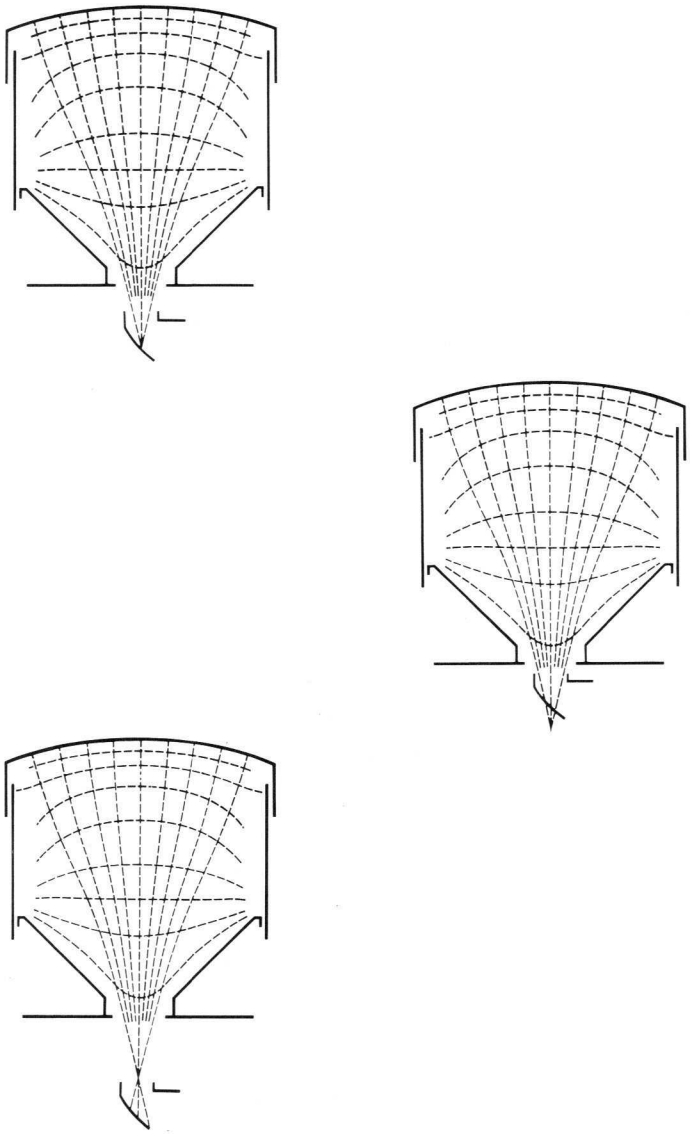

Fig. 4.7. Possible positions of the focus of the principal rays and the first dynode relative to one another. The tube considered is a 56 AVP (old model), and the faults are greatly exaggerated.

The transit-time spread

Here again, it is convenient to separate the variables and to assume that the component of the initial velocity normal to the cathode only alters the transit time and not the form of the trajectory, while the tangential component only alters the form of the trajectory without changing the time required for the electron to reach the first dynode S1. This is only a first approximation in the case of tangential initial velocity, which only involves a slight perturbation in the principal trajectory issuing from the same point on the cathode. Measurements on tubes 56 AVP, 58 AVP and XP 1020 have led to the following results:

1. The effect of an initial velocity normal to the cathode corresponding to an energy W_n of 0.4 eV does not change the point of impact on S1 appreciably, but reduces the transit time by a time Δt_n, equal to about 6×10^{-10} s for the 56 AVP, 5×10^{-10} s for the 58 AVP and 2×10^{-10} s for the XP 1020. The value of Δt_n is practically independent of the point of emission of the electron from the cathode.

$$\Delta t_n = -\sqrt{\frac{2m}{e}} \frac{\sqrt{W_n}}{E} \tag{11}$$

(in SI units, apart from W_n which is in eV), where m is the mass of the electron and e its charge, W_n is the energy corresponding to the initial velocity and E is the electric field at the cathode.

2. A tangential initial velocity corresponding to an energy of 0.4 eV shifts the point of impact by a certain distance (see Fig. 4.8) and changes the transit time, (generally negligible). The shift of the point of impact also depends to a certain extent on the point on the cathode from which the electron is emitted. Both define the radius of what we may call the "diffusion spot", i.e. the cross-section being taken at right angles to the beam at about the point where it impinges on S1 (see Fig. 4.8).

The shift of the impact point is 2.2 mm for the 56 AVP, 4 mm for the 58 AVP and 1.5 mm for the XP 1020, about the central principal ray.

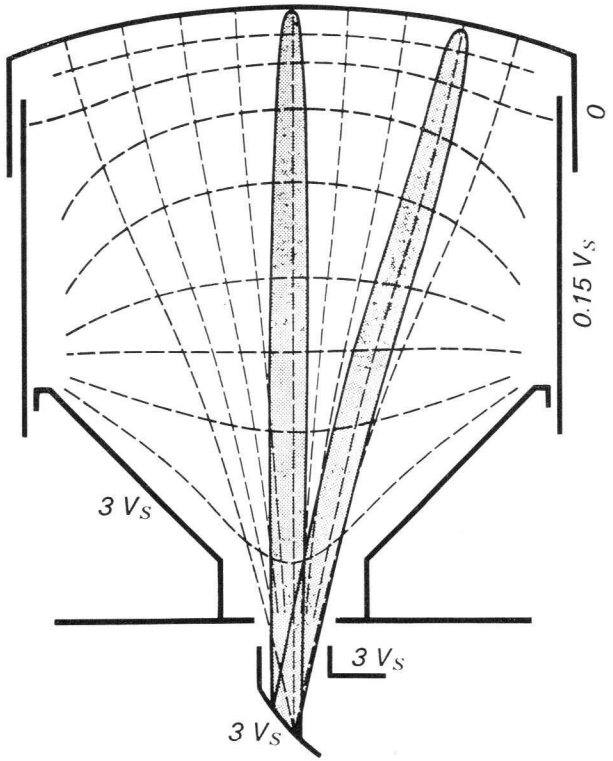

Fig. 4.8. (a) Broadening of the electron beams due to the tangential component of the initial velocity of the electrons in the 56 AVP (old model).

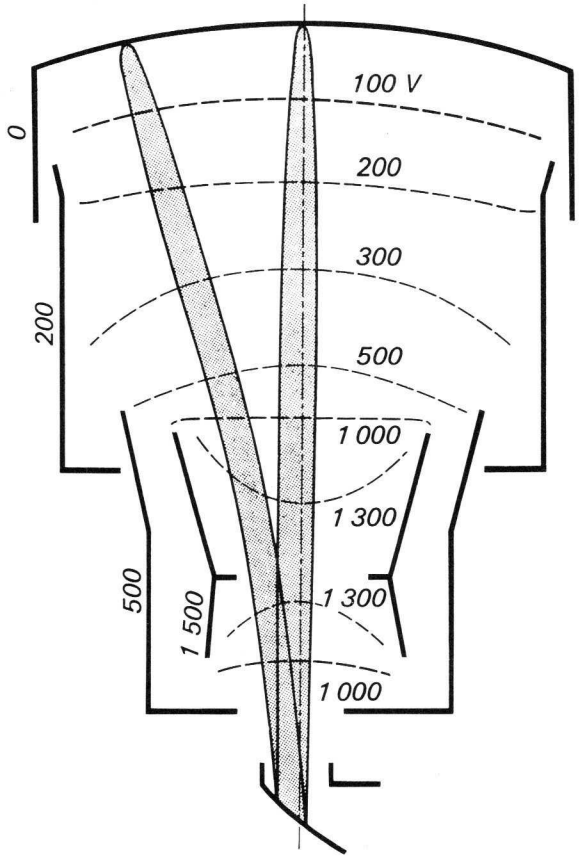

Fig. 4.8. (b) Broadening of the electron beams due to the tangential velocity of the electrons in the 58 AVP. The potentials of the electrodes are indicated on the drawing. The initial tangential velocity is taken as equivalent to 0.4 eV.

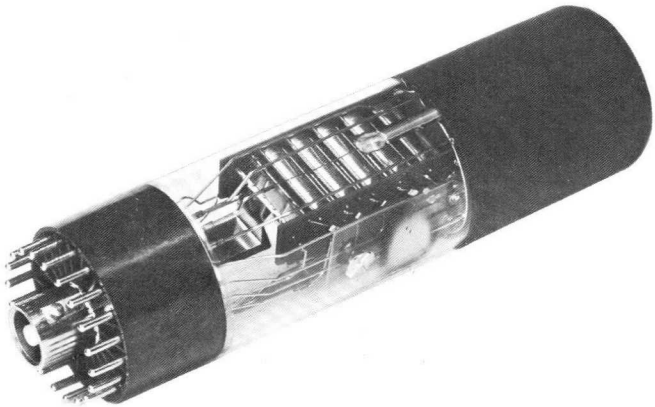

Fast response photomultiplier type XP1020
(approx. half full size)

Remedies for transit-time errors

Transit-time spread

Equation (11) shows that the effect of the initial velocities can be minimized by making the field at the cathode, E, as high as possible. This equation also shows that when the field E is uniform, the transit-time spread will be the same for all beams, no matter what their point of emission from the cathode.

The transit-time difference

The only way to correct for the transit-time difference is adjust the field distribution in the input optics successively until the desired result is obtained. When it is desired to make all the rays emitted by the cathode pass through a single focal point, one chooses the potential distribution approximately the same as that found between two concentric spheres. This explains why the surface of the cathode is generally spherical. Moreover, such a distribution satisfies the condition E is constant at all parts of the cathode, as we have mentioned above. Unfortunately, since the cathode is the outer sphere, E tends to have a low value on this slightly curved surface. This difficulty is overcome by the use of intermediate electrodes, which make it possible to keep the distribution of the lines of force more or less radial and the electron trajectories as linear as possible.

It is worth while stressing again here that the main object of improving the isochronism in the input optics (reducing the variance σ_{CS1}^2 of the transit times between the photocathode and the first dynode) is to reduce the variance σ_χ^2 of the overall transit time of the electrons in the photomultiplier (see equation (8)).

Description of the different input optics

Types derived from the photomultiplier 56 AVP[1]

The photomultipliers of the 56 AVP series have "triode" input optics consisting of three electrodes:
- the photocathode, k,.
- the accelerating electrode, acc,
- the focusing electrode, g1, arranged as shown in Fig. 4.9 (a).

[1] See Table 3.

The photocathode is spherical, for the reasons we have just given· The mean extraction field E of the electrons from the photocathode is defined by the potential of the accelerating electrode; as this electrode is electrically connected to the first dynode S1 of the multiplier, its potential also defines the energy of impact of the electrons on S1.

The electrode g1 makes the electric field at the surface of the photocathode uniform, so as to reduce the influence of the initial velocities of the electrons to the minimum. This makes the trajectories of the electrons much straighter, and concentrates them better on the first dynode. The potential of g1 is positive with respect to the photocathode, and is made

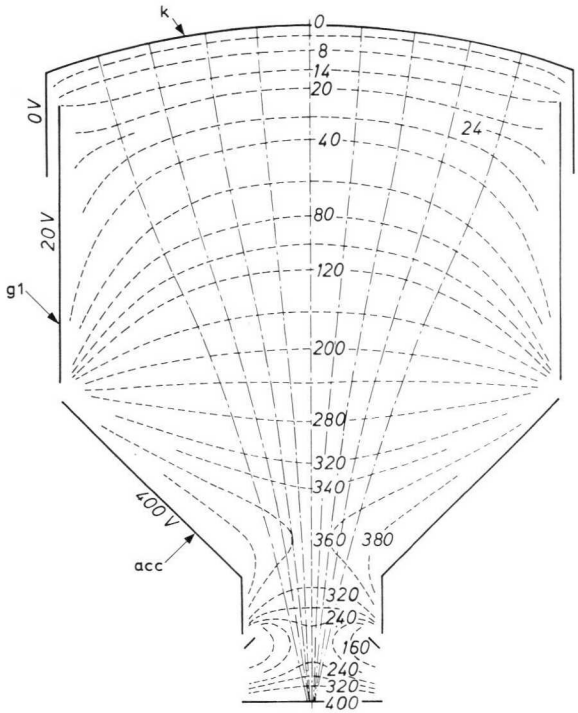

Fig. 4.9. (a) Equipotential lines in the input optics of the photomultiplier 56 AVP.
k = photocathode
g1 = first focusing electrode
g2 = second focusing electrode
acc = accelerating electrode

adjustable so that the conditions of maximum efficiency or uniformity of collection (maximum anode signal for a given luminous flux) can be found. The value about which the potential should be adjusted is about 0.15 times the inter-dynode voltage V_s.

The accelerating electrode (in the form of a truncated cone) accelerates the electrons and concentrates them on the first dynode. In order to reduce the influence of the initial velocities as much as possible, the potential of this electrode (and hence of S1) should be greater than or equal to 300 V.

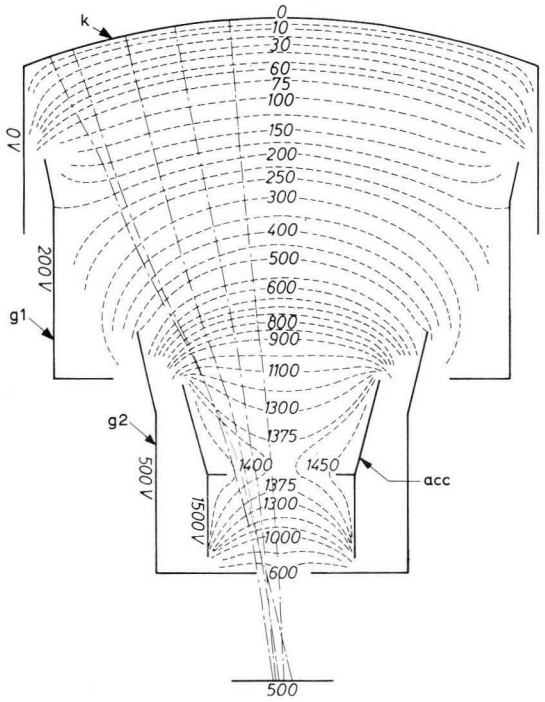

Fig. 4.9. (b) Equipotential lines in the input optics of the photomultiplier 58 AVP.
k = photocathode
g1 = first focusing electrode
g2 = second focusing electrode
acc = accelerating electrode

Types derived from the 58 AVP

These tubes have a much larger photocathode than those of the 56 AVP series, namely 110 mm in diameter compared with 42 mm. Now, since the values of the potentials applied to the electrodes clearly depend on the dimensions of the input optics we would have to multiply all potentials by about 2.5. The potential applied to the first dynode would then be of the order of 1 000 V, which is above the value corresponding to maximum secondary-emission coefficient of this dynode; (magnesium on oxidized silver) see Fig. 4.10. Moreover, this would make the supply voltage required for the photomultiplier excessively high. This means that we must look for a new geometry for the input optics.

The tubes have therefore been given tetrode-type input optics, (Fig. 4.9 (b)), a second focusing electrode g2 having been added. With this arrangement, the potential of the first dynode need only be raised to 500 V, while the accelerating electrode is given a potential of 1 500 V (taken from the tenth dynode of the multiplier). The second focusing electrode g2, the rear part of which is flat, is placed behind the accelerating electrode. It thus plays the role of a braking electrode, reducing the energy of impact of the electrons on the first dynode to a suitable value. This electrode is

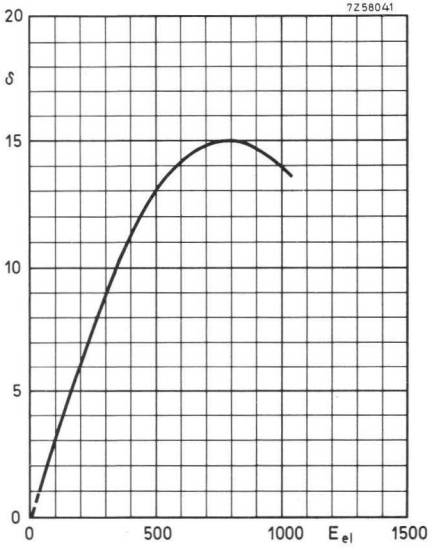

Fig. 4.10. The secondary-emission coefficient of a silver magnesium alloy as a function of the energy of the primary electrons.

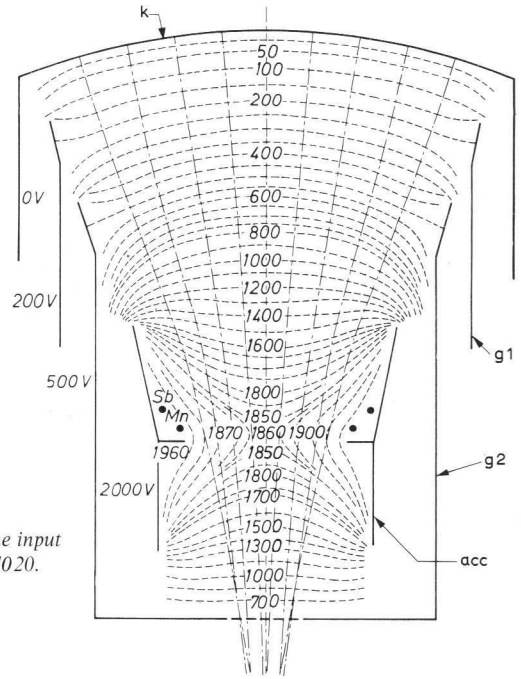

Fig. 4.11. Equipotential lines in the input optics of the photomultiplier XP 1020.
k = photocathode
g1 = first focusing electrode
g2 = second focusing electrode
acc = accelerating electrode

electrically connected to the first dynode. The focusing electrode also helps to improve the collection efficiency in the space in front of the accelerating electrode.

The potential of g1 should be adjusted by trial and error to the optimum value (about $2V_s$), according to the same criteria as for the triode optics.

Photomultipliers of the XP 1020 series have a photocathode the same size as that of the 56 AVP series, but they have tetrode input optics (see Fig. 4.11). This has made it possible to give these tubes a smaller spread in overall transit-time than the 56 AVP tubes, thanks to the higher electric field at the surface on the photocathode and a smaller spread of transit times between the dynodes S1 and S2. In other words the XP 1020 tubes are *faster*.

Fig. 4.9 and 4.11 show, apart from the form of the input optics for the 56 AVP, 58 AVP and XP 1020, some equipotential lines and principal trajectories of some electrons (i.e. trajectories followed by electrons with zero initial velocity).

4.3.2 Multiplier System

The causes of transit-time errors, and some possible remedies

Most of the spread in the transit times of electrons passing through the photomultiplier is produced by the multiplier. There are two main causes for this spread:

- the differences in the time required to cover the different electron trajectories possible between a given pair of dynodes;
- the variation in initial velocity, which increases still further the number of possible trajectories and changes the velocity with which the electrons travel along them.

The same problem occurs here as in the input optics, but in an even more serious form, because:

- the determination of a geometry giving isochronous principal rays (and compatible with all the other properties demanded of this structure) is a much more difficult matter than for the input optics;
- the initial velocities with which the secondary electrons are emitted are considerably higher than those for the photoelectrons;
- repetition of the effects involved over a large number of stages (14 in current models) increases the spread in transit times and in the geometry of the electron trajectories even more;
- finally, the induction current which precedes the actual inpact of the electrons from the last dynode on the anode serves to widen the pulse response even further.

The remedies applied to the input optics are clearly applicable to the multiplier too; in particular, it is valuable to look for a dynode geometry which leads to equal transit times for all trajectories, and produces the maximum (uniform) electric field at the surface of each dynode for a given potential difference.

However, apart from looking for improved dynode geometry, increasing the inter-dynode voltage V_s also helps to reduce the spread in transit time between the dynodes. It may be seen from equations (10) and (11) that:

1. for a given dynode geometry, the transit time of electrons emitted with zero initial velocity varies as $V_s^{-\frac{1}{2}}$.
2. in the beam created round a principal trajectory by the esistence of various possible initial velocities, the differences in transit time vary as the inverse of the electric field at the point of emission, i.e. as V_s^{-1}.

3. the width of these beams at any given point along their line of travel, and in particular at their point of impact on a dynode, varies as $V_s^{-\frac{1}{2}}$ to a first approximation.

It follows that increasing the voltage V_s leads to a reduction in the variance σ_{SS}^2 of the transit time of the electrons between two successive dynodes and hence, in accordance with equation (9), to a reduction in the "broadening" in time which the current pulse undergoes on passing from one dynode to the next.

However, increasing the inter-stage voltage also has other advantages:

1. The amplification is a stochastic effect, i.e. the width (ψ) of the output pulse corresponding to a given input signal is not fixed, but fluctuated about a certain mean value from experiment to experiment. The relative variance of the pulse width v_ψ decreases when the inter-stage voltage (and hence also the gain per stage) increases, as may be seen from equation(6).
2. Increasing V_s, i.e. the gain per stage, allows us to reduce the number of stages required for a given overall gain G. Reducing the number of stages automatically reduces the width of the output pulse, in accordance with equation (9).

Finally, it should not be forgotten that while the dimensions of the output pulse are affected by all stages of the photomultiplier, the fluctuations of the transit time of these pulses only depend on the first few stages of the multiplier together with the input optics.

The most effective way of reducing the variance of the overall transit time is thus to get rid of transit-time errors in the first few stages of the photomultiplier and to ensure high gains in these stages.

Description of the multiplier

We shall now consider in more detail the three main parts of the multiplier; the transition zone, the iterative structure and the collection space.

The transition zone

The coupling between the input optics and the multiplier is realized by the first few dynodes. These dynodes are given a special shape, the main function of which is to adapt the electron beam from the input optics to the new geometry of the multiplier, while losing as few electrons as possible in the process.

Fig. 4.12 shows the equipotential lines and principal electron trajectories in the transition zones of the 56 AVP (old model) and the XP 1020. In the new 56 AVP tubes, the dynodes of the transition zone are identical with those of the XP 1020.

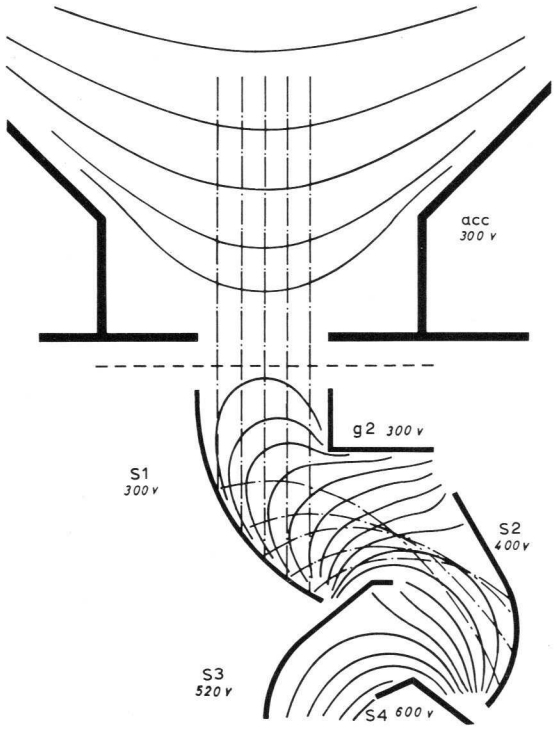

Fig. 4.12. (a) Equipotential lines and electron trajectories in the transition zone of the multiplier of the 56 AVP (old models, before No. 24310).

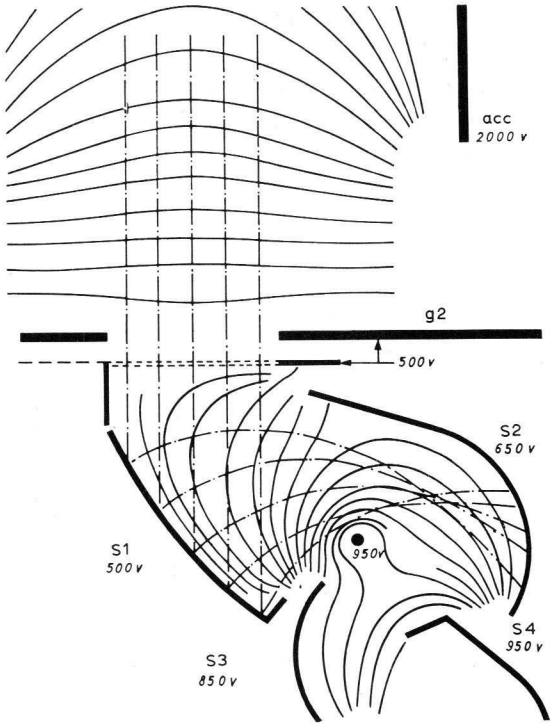

Fig. 4.12. (b) Equipotential lines and electron trajectories in the transition zone of the multiplier of the XP 1020.

The iterative structure

Fig. 4.13 (a) shows a cross-section through the dynodes in the iterative part of the multiplier of the 56 AVP or the XP 1020, together with the net of electron trajectories. This figure also shows the straight wire electrodes used between the dynodes to increase the extraction field at the surface of the dynodes and to improve the focusing of the electrons.

The focusing properties of this structure have been illustrated in Fig. 4.13 (b). We see there that the bundle of electron rays is gradually concentrated as it passes through the multiplier from the first dynode to the last. This focusing limits the transit-time errors by successively bringing all electron trajectories closer to a certain mean path, the fluctuations about which are finally very slight.

Finally, on going from the 56 AVP to the XP 1020, the number of dynodes is reduced from 14 to 12, while the average inter-stage voltage is increased from 120 V to 200 V. It should also be remembered that the voltage applied between the photocathode and the first dynode is larger than that between the dynodes, being about 350 V for the 56 AVP and 500 for the XP 1020.

The collection space

Towards the end of the multiplier, the geometry of the electrodes is deliberately made different from that of the recurrent structure. This is because the form of the electrodes in this region must allow them to:

- collect all the charge;
- reduce the space charge there to well below the level corresponding to the maximum pulse amplitude to be expected;
- reduce, and equalize as far as possible, the transit times of the electrons during the last part of their journey;
- reduce the electromagnetic coupling between the anode and the neighbouring electrodes, and between the anode and the electron beams other than those producing the useful signal.

These aims are partially compatible, so the choice of the geometry of the terminal zone is actually a compromise.

The collector proper consists of a grid placed as close as possible to the last dynode, so as to reduce the transit times of the electrons in this last stage to the minimum. However, once the geometry of the collection space has been defined, the distribution of the voltages applied may be left to

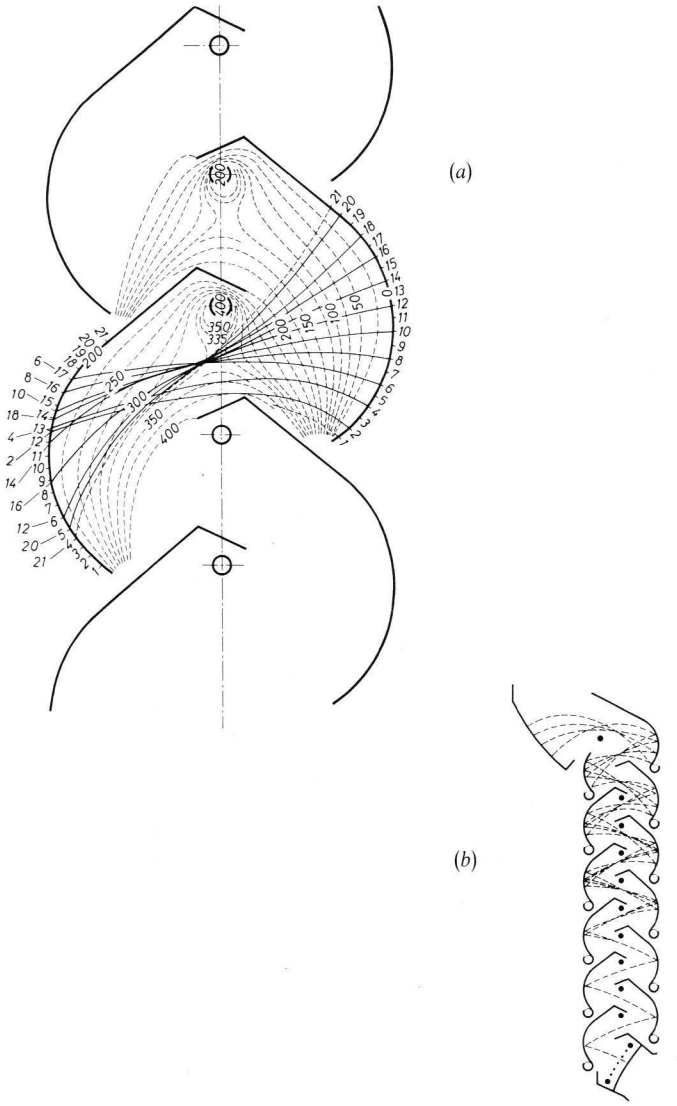

Fig. 4.13. Construction of the multiplier of a fast photomultiplier:
(a) detail of dynodes,
(b) overall view.

the discretion of the user to a certain extent, since there is in fact no solution which completely meets all requirements simultaneously.

Fig. 4.14 shows in detail the geometry of the collection space photomultipliers 56 AVP and 58 AVP. These two types both have 14 dynodes; the last one, S14, provides a measure of electrostatic screening around the collector.

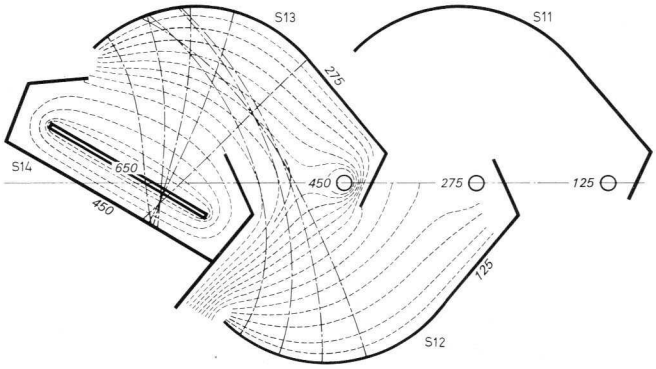

Fig. 4.14. Geometry of the terminal collection region in photomultipliers of the types 56 AVP and 58 AVP (the values of the potentials given were measured relative to S11).

Fig. 4.15 shows the current pulses obtained at the anode of a photomultiplier type 56 DVP with two different methods of wiring the last dynode. In the first case, the dynode S14 is decoupled by means of a 1 nF capacitor. It may be seen from Fig. 4.15 (a) that in this case, even when the tube is wired very carefully, oscillation occurs at the end of the pulse. This oscillation is due to the inductance of the connection to the last dynode. This difficulty can be avoided by inserting a 50 Ω demping resistance into the circuit of this dynode. As may be seen from Fig. 4.15 (b)[3] this effectively suppresses the oscillation.

Photomultipliers of the XP 1020 family have two major advantages over those of the 56 AVP family:

- the fluctuations in transit time in the last stage of the multiplier have been reduced;
- the anode impedance of the tube has been better matched to the associated electronic circuits.

[3]) This resistance is built into the base of the tube starting from No. 31000 of type 56 AVP, No. 5677 of types 58 AVP and XP 1040 and No. 144 of type 60 AVP.

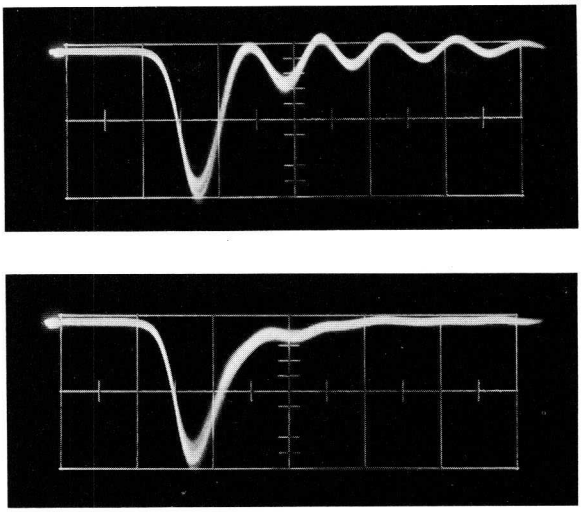

Fig. 4.15. Anode pulses of a photomultiplier of type 56 DVP, obtained by illuminating a point on the photocathode by the spark generator SL 109[1], *with voltage distribution B'* [2] *and HT voltage 2500 V:*
(a) circuit of dynode S14 decoupled by a 1-nF capacitor;
(b) 50-Ω series resistance in the circuit of dynode S14.
Ordinate scale: 100 mA per main division
Abscissa scale: 5 ns per main division

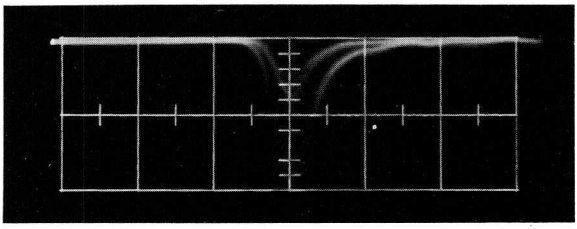

Fig. 4.16. Anode pulses of a photomultiplier of type XP 1021, obtained by illuminating a point on the photocathode by the spark generator SL 109[1], *with voltage distribution B'* [2] *and HT voltage 2500 V.*
Ordinate scale: 100 mA per principal division
Abscissa scale: 5 ns per principal division

[1] See Appendix 4.
[2] For the definition of distribution B', see Section 5.1.

We shall consider the second point first. The photomultiplier is normally followed by a coaxial cable which has to carry the output pulses without attenuation or distortion over distances which may be quite large. It is an obvious idea under such circumstances to equip the photomultiplier with a coaxial connector so that the cable can be connected without any trouble. It is also necessary to design the last few electrodes so that they are gradually adapted to the coaxial line. The photomultipliers XP 1020 and XP 1021 have been equipped with 100 Ω and 50 Ω coaxial outputs respectively.

Concerning the first point mentioned above, photomultipliers type XP 1020 have a supplementary grid parallel to the collector grid, the wires of the two grids being made parallel to one another, on order to improve the pulse response. However, part of the improvement in transit time and in pulse form is due to the coaxial structure used.

This supplementary electrode g3 is given a voltage near that of the last dynode. The form of the anode pulses produced by photomultipliers types 56 AVP and XP 1020 may be compared by inspection of Fig. 4.15 and Fig. 4.16 respectively. This supplementary electrode can also be used as a control electrode, allowing the amplitude of the anode pulses to

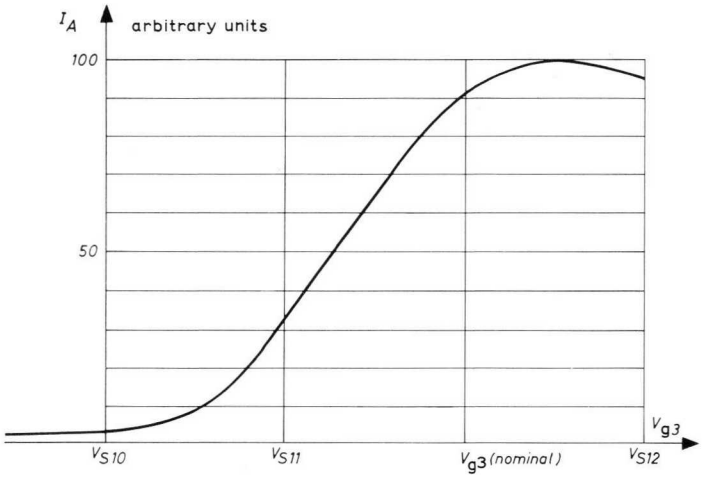

Fig. 4.17. Anode sensitivity characteristic of an XP 1020 photomultiplier as a function of the potential of the screen grid g3.

be adjusted without it being necessary for the incident luminous flux or the HT supply to be altered. The control characteristic of this grid is shown in Fig. 4.17.

The development from the 56 AVP to the XP 1020 series, involving a reduction in the number of stages, changes in the last stage, and adaptation of the collector for use with a coaxial line, has made it possible to reduce the rise time of the anode pulses from 2 ns to less than 1.9 ns, with a mean gain of 10^8.

However, all types of photomultipliers are still undergoing further development, and it may be expected that later models will all have very wideband matching of the anode to the coaxial cable, together with a drastic cut in the inductances of the connections, at least in the last few stages, giving the kind of improvement seen between Fig. 4.15 (a) and 4.16.

In Section 4.5, we shall discuss a new photomultiplier type XP 1210 which embodies many of the above-mentioned advantages.

4.4 Performance of some Fast Response Photomultipliers

The modifications and improvements made in both the input optics and the multiplier systems of recent years have led to present performances, summarized in Table 2.

Table 2. Summary of Principal Characteristics.

type	rise time (ns) [1]	half-height width (ns) [1]	transit-time difference (ns) [2]	supply voltage (V)
56 AVP	2	< 4	< 0.5	2500
58 AVP	2	< 4	1	3000
XP 1020	< 1.8	< 3	< 0.2	2500
XP 1210	1	1.5	< 0.2	5000

[1]) When the whole photocathode is illuminated by a very brief light pulse from an SL 109 spark generator (see Appendix 4).

[2]) Difference between the transit time of an electron from the centre of the photocathode to the anode and from the edge of the photocathode to the anode.

4.5 Photomultiplier XP 1210

The photomultiplier XP 1210 marks a new step forward in improved speed of response; this type has a rise time of only 1 ns. Its most striking characteristic is the novel technology used for its envelope, and the way in which the electrodes are mounted inside this envelope.

The XP 1210 is made by the technique of sealed stacked discs, and it has a coaxial output similar to that of the XP 1021. The two main aims of this special design are:

- improvement of the accuracy of the positioning of the electrodes relative to one another;
- improved protection against ions and light travelling back down the tube, and against cold emission.

This new technology also gives a considerable reduction in the parasitic inductance of the dynode connections. At the same time, a fair degree of decoupling is automatically introduced petween the stages.

Fig. 4.18 shows a sectional view of the XP 1210; details of the input optics, the multiplier and the output system may be clearly seen.

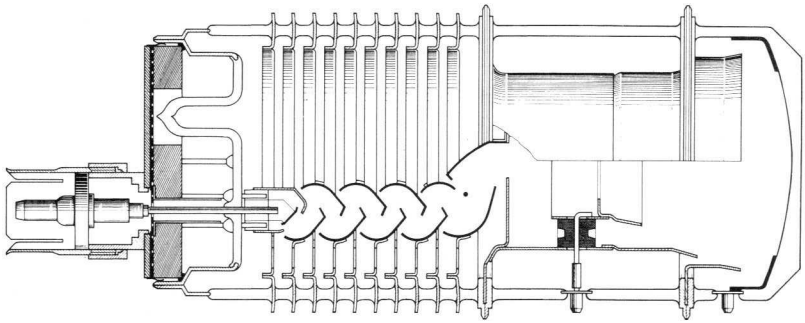

Fig. 4.18. Basic construction of the photomultiplier XP 1210.

4.5.1 Improving the Rise Time

As we have indicated above, the rise time can be reduced by decreasing

- the transit time spread of the photoelectrons and the secondary electrons in the various stages of the photomultiplier;
- the duration of the induction current produced at the collector by the arrival of the electrons emitted by the last dynode.

Increasing the inter-stage voltage

The input optics of the XP 1020 gives transit-time errors of the order of 2×10^{-10} s, i.e. quite low enough to the justify using these input optics with a faster multiplier than that found in the XP 1020.

In the multiplier, the electrons pass through one region in which they are accelerated and one in which they are decelerated on travelling from any dynode to the next. The differences in transit time are always produced when the velocity of the electrons is lowest, i.e. at the start of the acceleration period. The transit-time errors could thus be appreciably reduced by increasing this acceleration, i.e. by increasing the extraction field at the surface of the dynode.

The solution chosen for the XP 1210 was thus simply to increase the voltages applied to the multiplier, which has the same basic structure as that of the XP 1020. We have seen that this increase in voltage will always improve the focusing of the multiplier, and at the same time increase the secondary-emission coefficient so that the number of dynodes can be reduced. With 10 dynodes, a gain of 10^7 corresponds to a secondary-emission coefficient δ of the order of 5 ($5^{10} = 10^7$). Now, with the dynodes used in the 56 AVP and the XP 1020, this value of δ corresponds to inter-stage voltages V_s of the order of 200 V. It is therefore to be expected that a multiplier with 10 stages and inter-stage voltages of the order of 250 V will have rise time of about 1 ns. Because of difficulties which may arise in connection with the activation of the dynodes, it is advisable to choose the value of V_s even higher (up to a maximum of 300 V); this means that a very high supply voltage (4 to 5 kV) is required.

Regarding the coupling between the input optics and the multiplier, the largest transit-time errors are produced in the first stage, between the dynodes S1 and S2. The rise time of this stage is about 1 ns in the 56 AVP, but less than 0.5 ns in the XP 1020. In the latter case, the overall rise time of a 10-stage multiplier, associated with the input optics of the XP 1020, should be of the order of 1 ns.

The disadvantage of increasing the HT voltage is that there is a tendency towards higher dark currents due to the luminescence effects. However, if the voltage is distributed uniformly along the tube, so that very high voltage gradients are avoided, and if the interior of the tube is divided up by screens so that ions and light cannot travel backwards along the tube to the cathode, the dark current can be kept down to a reasonable value (10^{-15} A.cm^{-2}, with reference to the cathode).

The collection space

The anode of photomultipliers for use in nuclear physics is generally made as a grid, situated very near the last dynode. In the XP 1020, on the other hand, the collector is made in the form of a disc.

It will be obvious that a collector of this type cannot be placed very close to the last dynode. It must therefore be screened, i.e. given a low capacitance with respect to the last dynode, so that the electrons emitted from the last dynode do not give rise to an appreciable induced current before they arrive. The screening placed round the anode should form, together with the anode, the start of a matched line for the transmission of the signal. This means that the capacitance between the screening and the collector should also be low.

These conditions have been satisfied in the XP 1210 by means of a comprise between the various requirements involved: the collector has been made big enough to capture all the electrons, and close enough to the screening to reduce the transit time of the electrons from the one to the other.

The disadvantage of a collector of this type is that it does not give as high an extraction field as that from the grid at the last dynode, which limits the range of linearity to 75–100 mA. However, with a gain of 10^7 such currents correspond to pulses containing as many as 100 electrons at the photocathode.

The inductance of the connections

The inductance of the connections between the anode and its screening should be such as to give a matched line with a characteristic impedance of 50 Ω. This value, which is standard in high-frequency electronics, has been chosen to reduce the influence of parasitic capacitances to the minimum.

Concerning the other connections, their impedance should be as low as possible; in other words, the capacitance between neighbouring dynodes, or between dynodes and earth, should be as high as possible with respect to the inductance of the connections. The XP 1210 is constructed so as to meet this requirement; the capacitance between two successive screens supporting the dynodes is of the order of 20 pF, and the inductance has been reduced basically to that of the few soldered joints involved.

4.5.2 Description of the XP 1210

The photomultiplier XP 1210 thus comprises:
- the input optics and transistion zone of the XP 1020;
- a multiplier with 10 dynodes similar to those of the XP 1020;
- a collector formed of a solid disc surrounded by screening.

The envelope is formed by a stack of glass and metal discs, sealed together in three units which are finally joined by argon-arc welding after assembly of the tube.

All the electrodes of the input optics (apart from the accelerating electrode) and of the multiplier are supported by the metal rings which form part of the envelope. The tube is protected against ions and light travelling backwards towards the cathode by means of screens soldered on the rings; the dynodes are in fact fixed to these screens. For technological reasons, the wire-shaped focusing electrodes in the multiplier have been omitted, without this having much effect on the focusing of the electrons. Only the focusing electrode between dynodes S1 and S2 has been retained; but this is connected to dynode S4.

The anode output is in the form of a standard 50 Ω coaxial socket.

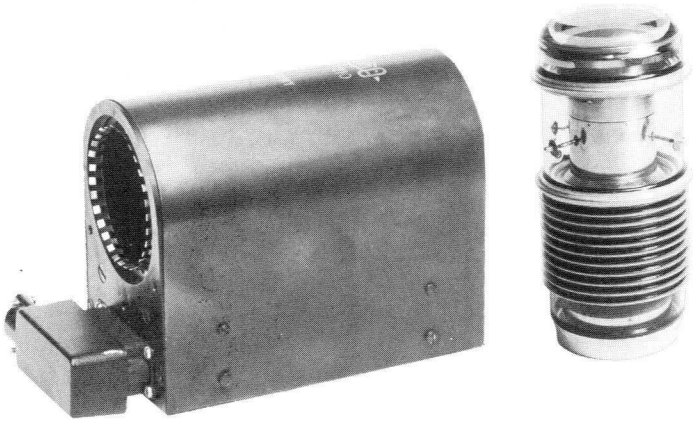

Fast response photomultiplier type XP1210 with its socket type 56 040 (approx. half full size)

5 Achievement of High Peak Currents in Pulses

5.1 Improving the Linearity of the Current

One of the most important properties demanded of modern photomultipliers is that they should be able to deliver very high current peaks for short periods of time. This goes hand in hand with the high speed of these tubes, since it allows the production of signals which can be used directly (without preliminary amplification) in low-impedance circuits.

For a long time, the photomultiplier only gave a linear, reliable response up to currents well below one milliampere. During the past decade, the range has been extended to some tens of milliamperes, and is now tending towards one ampere. This tendency towards higher current levels has been dictated by the developments in high-energy physics. At present, certain photomultipliers even give peak currents of several amperes (3 to 5 A) in the anode pulse.

It is a fortunate fact that those features which give a high speed of response, also give high anode currents; these two requirements are thus quite compatible. At present, the main factor limiting the linearity of the current is the space charge. If possible, the useful surface area of the dynodes should be increased, while still retaining the good transit-time properties and speed of response; but above all the electric field should be increased which means that higher voltages should be used.

On the other hand, excessive voltage variations between successive stages should be avoided. The inter-dynode voltage V_s should be successively multiplied by a factor k, (between 1 and 2), starting from the dynode at which the current reaches its limiting value (100 mA for fast photomultipliers). If this increase starts at the ith stage, the voltage between the last dynode and the one before it will be $V_s \times k^{n-i}$, where n is the total number of dynodes. The larger k is, the later the stage at which the voltage increase should be started so as to ensure that the maximum permissible inter-dynode voltage (500 V for fast photomultiplier) is not exceeded. The value of n is thus defined by the relation

$$V_s \cdot k^{n-i} < V_{s\max} \cdot$$

For example, if $V_s = 100$ V, $V_{s\max} = 500$ V and $k = 2$, we find $n > 12$ for a photomultiplier with 14 dynodes.

With $k = 1.2$, the increase in the voltage can be started at the sixth stage. Voltage distribution B, quoted in the data sheets of the 56 AVP, is an example of this. This allows the linearity range of the tube to be extended to 300 mA. However, distribution B′ ($k = 1.5$, $n = 12$) gives a better pulse response.

In photomultipliers which have been specially designed for high peak currents (up to 5 A), the voltage distribution between the dynodes is modified so as to reduce the space charge as much as possible. In these tubes, not only is the inter-stage potential difference increased, but the electron beam is also made less concentrated in the last few stages, which naturally leads to much less regular voltage distributions. In the next section, we shall consider a photomultiplier designed to give both very fast response and excellent linearity up to high currents. This tube has the type number XP 1143.

5.2 Photomultiplier type XP 1143

This tube has been developed to reproduce without distortion extremely short light pulses (with durations of the order of one nanosecond) of high intensities of illumination.

The 56 AVP already gave good linearity in pulse operation (up to 300 mA, in a classical set-up). However, the linearity range of this tube *is* limited, mainly by reason of its high gain. We therefore had to design a new photosensitive element, intermediate between that of the 56 AVP and a photoelectric cell, with a gain of 1 and linearity up to several tens of amperes. This development led to the XP 1143 photomultiplier, the principal characteristics of which are:

linearity (5%)[1]	up to 5 A in pulse operation
gain	10^4 to 10^5
rise time	< 1 ns
transit time	10 ns
half-height width	< 2 ns.

[1] The linearity (5%) is defined as the anode current in amperes up to which the curve of anode current as a function of luminous intensity at the photocathode does not depart from a straight line by more than 5%.

In order to get these high performances, we had to reconsider the entire construction of the photomultiplier. We shall now go through the various parts of the tube in turn, showing how the demands made led to modifications.

The photocathode

We have already mentioned the advantages of widening the electron beam in the multiplier in the interests of better current linearity. This widening can be obtained by modifying the focusing of the tube.

The focusing at right angles to the axes of the dynodes can be modified by slight adjustments to the profile of these electrodes. The focusing in the plane of the axes is produced by the input optics, which is difficult to modify.

In the XP 1143, we have widened the electron beam, particularly in the first few stages, by the use of an *opaque photocathode* deposited on a conducting support with the form of the first dynode and, in fact, replacing it (the input optics being omitted). This solution also improves the speed of the tube; since the input optics are not there, the overall transit-time is considerably less.

The photocathode is formed by a thin film of Sb–Cs deposited on a metallic support; it is inclined at 45° to the input window of the tube. Its spectral response is of the type S4 (see Fig. 2.2).

The multiplier

After the omission of the input optics, another radical change in the photomultiplier in the interests of a higher current linearity consists of a delibrate reduction in the number of dynodes and an increase in the useful surface area of each dynode. Most of the structural characteristics of the multiplier of the XP 1143 are identical with those of the 56 AVP, for example dynode profile, choice of material for the secondary-emission layer; but the number of dynodes has been reduced from 14 to 6, and the axial length of the dynodes has been doubled, being 50 mm in the XP 1143 compared to 25 mm in the 56 AVP and the XP 1020. We may also mention the presence of wire-shaped accelerating electrodes in the multiplier, which are connected to the inner wall of the tube so as to reduce space-charge effects to a great extent.

The increase in the dimensions of the electrodes and the great rigidity required for their supporting rods have led to a complete rearrangement of the electrodes within the tube, which now has a side-window.

The output stage

The last big improvement made in the XP 1143 consists of a complete remodelling of the output stage.

As we have mentioned, conventional tubes (with the exception of the XP 1210) have their anode in the form of a grid, which allows the primary electrons emitted by the last dynode but one to pass through, while capturing the secondary electrons emitted back down the tube by the last dynode (Fig. 4.14). This form of anode gives rise to a parastic signal superimposed on the useful signal at high currents, which thus stands in the way of both fast operation and good linearity.

This effect is due to the collector grid being too transparent to the secondary electrons emitted by the last dynode. Some of these electrons can thus pass through the grid without being collected and travel in the

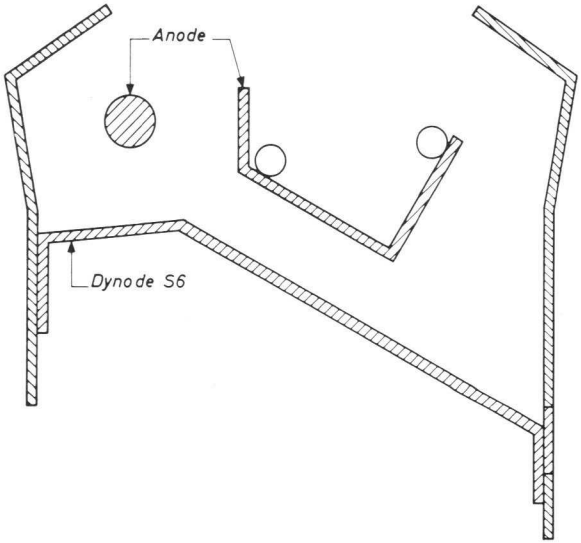

Fig. 5.1. Output stage of an XP 1143 photomultiplier.

direction of the last dynode but one until they are stopped by the electric field; the dynamic accelerating field present at high current levels can now send these electrons back through the grid, so that they fall again on the last dynode, giving rise to a fresh emission of secondary electrons.

This led us to try to make the collector grid of the XP 1143 practically non-transparent in the direction from the last dynode to the anode. We have achieved this by using an opaque anode with a slit in it (Fig. 5.1).

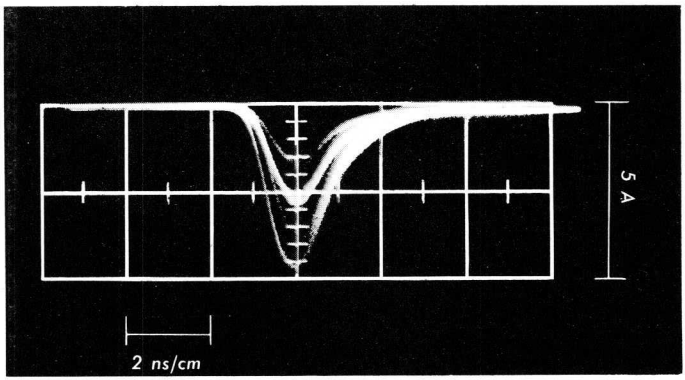

Fig. 5.2. Response of an XP 1143 to very brief light pulses of different intensities.

The primary electrons emitted by the last dynode but one (S5) are focused on this slit, so that they can pass through freely, while the form of the last dynode (S6) has been chosen so as to ensure practically total collection of the secondary electrons it emits. The output stage has also been matched to a 50 Ω coaxial line, terminated in a socket.

These various improvements made in the XP 1143 have led to remarkable performances in terms of speed and linearity. Fig. 5.2 shows the output pulses produced by the tube in reponse to very brief light pulses of different amplitudes, while Fig. 5.3 shows the linearity characteristic of the tube measured with respect to a reference photomultiplier operating in its linear range.

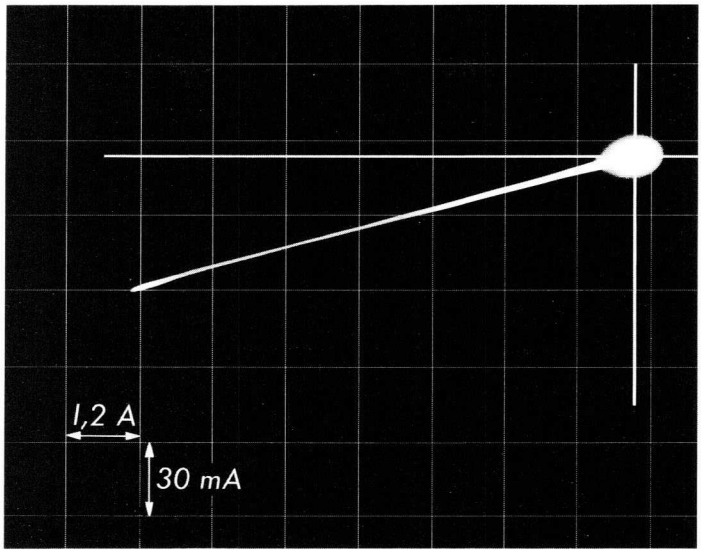

Fig. 5.3. Linearity characteristic of the XP 1143 photomultiplier. The linearity is investigated by comparing, on an XY oscilloscope with identical channels, the anode pulse from the photomultiplier under investigation and the anode pulse from a reference photomultiplier, known to be working in its linear range.
Ordinate: reference pulse amplitude (channel Y)
Abscissa: measured pulse amplitude (channel X)
The characteristic given here shows that the range of linearity (5%) extends to a peak current of about 7 A.

6 Fast Response Photomultipliers in Nuclear Physics

6.1 Measurement of High-energy Particle Velocity

Large particle accelerators produce high-energy particles which may have to be detected, identified or separated. The two detector types most widely used are Cerenkov counters and scintillation counters, as these both have the very fast response required.

The identification of the particles in a secondary beam is based on the determination of their charge and their mass. At present, the mass m of the particles is derived from measurement of their momentum p and their velocity which are related by the expression:

$$p = m\beta\gamma c$$

where $\beta = u/c$ is the ratio of the velocity of the particles u to the velocity c of light *in vacuo*, and

$$\gamma = \frac{1}{\sqrt{1-\beta^2}}.$$

For charged particles, the momentum p is measured by magnetic analysis of the particle beam, and the velocity u is deduced from the time the particles take to cover a fixed distance l.

6.1.1 Measuring Velocity from the Time of Flight

The velocity of the particles may be measured with the aid of two scintillation counters or Cerenkov counters placed in the beam a distance s apart, this distance being known as the *flight path.*

The velocity of each particle is measured with respect to that of light, i.e. as:

$$\beta = \frac{u}{c} = \frac{l}{ct}$$

where t is the time between the pulses from the two counters.

If we denote the root mean square error involved in the measurement

of the time of flight t by σ_t, then the minimum time which can be measured (the resolution time) is:

$$\Delta t \approx 2\sigma_t$$

The value of σ_t will be a function of the fluctuation of the registration times t_1 and t_2 of the particles in the counters 1 and 2 which define the flight path.

In general, the registration time of a particle in a counter is defined as the time of appearance of the centre of gravity of the output pulse produced by the first N_e photoelectrons. This definition avoids errors due to fluctuations in the amplitude of the pulse and reduces the resolution time to the minimum which is defined by unavoidable errors in the detector and the photomultiplier.

Fast response photomultipliers are particularly suited to measurements of this type, because of their high speed of response, the brevity of their output pulses and the low fluctuation of their transit times.

Scintillation counters

When a charged particle enters a scintillator, a flash of light is produced the intensity of which is approximately given by the expression:

$$I_e = I_{eo} \cdot e^{-t/\tau}$$

where τ is the characteristic decay time of the scintillator. For polystyrene scintillators (type SPF), this time constant amounts to a few nanoseconds (about 4×10^{-9} s). This light forms the input signal for a photomultiplier.

Now we have seen, the form of the output pulse produced by the photomultiplier varies from one particle to the next. This is due to the finite number of photons emitted and the fluctuations in the transit times of the electrons in the photomultiplier. The output information must thus be processed so as to obtain the maximum possible accuracy for the measurement of t_1 and t_2. For this reason, the times t_1 and t_2 are defined as the mean times of arrival at the anode of the photomultiplier of the N_e first photoelectrons, N_e being chosen in such a way as to minimize the fluctuations in the measured time.

The emission of the photoelectrons follows the law:

$$I_e(t) = \frac{\overline{N}_e}{\tau} \cdot e^{-t/\tau},$$

where $\overline{N}_e$ is the mean number of photoelectrons emitted per scintillation and τ is the decay time of the scintillator. It may be shown that if we want to reduce the variance of the measured time (mean time of collection of the first N_e electrons), we must reduce the value of the ratio $\tau/\overline{N}_p$. This means that we must choose a scintillator with the best ratio of the number of photons emitted to the decay time. On the other hand, we must ensure that the transfer of light from the scintillator to the photomultiplier is as efficient as possible, so as to increase $\overline{N}_p$.

The photomultiplier plays a role here by virtue firstly of the sensitivity of its photocathode and secondly of the factor $\sigma^2{}_\chi$, the value of which is given (see p. 44 and Appendix 3) by:

$$\sigma_\chi^2 = \sigma_{CS1}^2 + \frac{\sigma_{SS}^2}{g-1}\left(1 + \frac{2}{g}\right).$$

This factor represents the variance of the time at which the centre of gravity of the photomultiplier output pulse occurs. The first term, σ_{CS1}^2, the variance of the transit time between the photocathode and the first dynode, is the most important. However, the second term, representing the inter-dynode fluctuations, is not negligible. This term is due mainly to the first few stages of the multiplier, since the relative variance of the transit time at a given stage is inversely proportional to the square root of the number of electrons involved.

As we have seen, minimization of the above fluctuations leads to the minimum variance in the overall transit time (σ_χ^2) and hence to the maximum relative accuracy of the measurements. When a fast response photomultiplier is used together with an SPF scintillator it has proved possible to obtain a resolution time of the order of 5×10^{-10} s.

Cerenkov counter

Cerenkov light is emitted in all transparent media, no matter what their nature, by any charged particle with a velocity u exceeding c/n, where:

c is the velocity of light *in vacuo*, and

n is the refractive index of the medium.

The light emitted in this way has the character of a shock wave; it is therefore emitted at a constant angle to the trajectory of the particle, the value of this angle being given by:

$$\cos\phi = \frac{c}{n} \times \frac{1}{u} = \frac{1}{\beta n}$$

The light emitted is polarized. Its chromatic intensity I per unit bandwidth $\Delta\lambda$ only depends on the charge Q of the particle and the angle of emission, i.e. on the incident velocity. The number of photons emitted per unit wavelength by a radiator 1 cm thick is given by:

$$\frac{dN_p}{d\lambda} = \frac{4\pi^2 e^2 Q^2}{hc\lambda^2} \sin^2 \phi ,$$

where h is Planck's constant.

This equation shows that, apart from the sensitivity of the photocathode and the transparence, the photoelectric current is larger as the wavelength transmitted is shorter. This shows that it is advantageous to use photomultipliers with a window of fused quartz, which is transparent to ultraviolet. A glass window of the same thickness would give an appreciable lower current, because of the absorption in the near ultra-violet (see Section 3.1).

The light emitted by a Cerenkov radiator is of low intensity (about 20 times less than that emitted by a plastic scintillator of the same dimensions) but its rise time is extremely short; indeed, the duration of the light pulses is almost entirely due to the effects inevitably associated with the propagation of light in the radiator. This allows very high counting rates to be obtained when dealing with pulsed beams.

Using a set-up comprising two Cerenkov counters for the separation and identification of π^+ mesons and protons and of π^- mesons and antiprotons in a secondary beam, a resolution of better than a nanosecond (7×10^{-10} s) has been obtained.

6.1.2 Measuring Velocity by Cerenkov Effect

Threshold counters

The light emitted by the Cerenkov effect can be used in a number of ways for the measurement of the velocity of a particle. It follows from the angular relation given above that the threshold for the emission of the light is reached at $\beta = 1/n$. This property can be made use of for selection of particles in a certain velocity range, since a photomultiplier will only give a pulse when the particle velocity exceeds a limiting value determined by the refractive index chosen. In principle, a similar counter set to another

threshold allows us to determine whether the velocity of the particle lies within two fixed limits.

However, this method has disadvantages. The emission near the threshold (i.e. for ϕ near to zero) is very low in intensity. Depending on the experimental conditions and the sensitivity of the photomultiplier, the counter will only start to deliver pulses when the velocity of the particle exceeds the threshold velocity $u = c/n$ by a small amount (which is basically variable and ill-defined).

During experiments on the capture of μ^- mesons by carbon, a threshold counter formed by a water radiator and a fast response photomultiplier was used to eliminate π^- mesons from the beam of μ^- mesons.

Differential velocity-selection counters

Another way of measuring the velocity of a particle is provided by the fact that the Cerenkov light emitted is distributed in a cone, at a constant angle to the trajectory of the particle in question. If particles of the same velocity, following paths which were parallel or slightly divergent, pass through a transparent medium, then an observer looking in the direction of the incident particles would be able to see a ring of light each time a particle passes. This ring appears in a fixed direction, which does not depend on the position of the particle or on that of the eye of the observer. The low intensities involved, and in particular the rapidity of the effect, in fact make this phenomenon *invisible to the human eye*, but it can be detected by a photomultiplier.

A camera focused to infinity and pointed at the radiator will focus all the rays making a certain angle with the initial trajectory in an annular image, the radius of which depends on the velocity of the incident particle as follows:

$$R = F \tan \phi = F\sqrt{n^2\beta^2 - 1}\,,$$

where F is the focal length of the camera.

If a photocathode fitted with an annular diaphragm of suitable diameter is placed in the focal plane, only the particles with a given velocity will produce a pulse in the photomultiplier. This principle is made use of in differential velocity-selection counters based on the Cerenkov effect.

6.2 Studies on Heavy High-energy Particles

Certain problems of nuclear physics for which a linear detector with a very low resolution time (a few nanoseconds) seems indispensable can be solved with the aid of a scintillator consisting of a sample of rare gas, together with a fast response photomultiplier. Rare gases are characterized as scintillators by the very short life of the luminescence and by the great linearity of their response as a function of the total energy given up the gas by the incident particle.

For example, the luminescence of xenon is characterized by a very low time constant (about 2.2 ns), equal to the life of the excited states of the gas. Measurement of this life is a straight forward application of a fast response photomultiplier.

The study of nuclear reactions involves a certain number of heavy particles, which have very large specific energy losses. This is the case, in particular, with the fission ions, for which dE/dX can reach 70 MeV per cm in argon. The response of the scintillator used must thus be linear over a very wide energy range. Since, moreover, the ions are often accompanied by an intense flux of lighter particles (electrons or alpha particles), the life of the luminescence produced by the scintillator should be as short as possible if we are to avoid a pile-up of pulses at the output of the photomultiplier.

Gaseous scintillators, with their very linear response over a wide energy range and the low time constant of their luminescence, are thus invaluable for the detection of heavy ions and neutrons in nuclear physics.

Use of a gaseous scintillator with a fast response photomultiplier allows resolution times of the order of

$$\tau = 5.10^{-9}\ s$$

to be obtained; this is about 100 times less than that given by a classical fission chambers.

Such combinations have made it possible to study the spontaneous fission of the transuric elements, the half-lives of which are very brief (for example, americium 241 emits 10^8 particles per second per mg). Resonances in the effective nuclear cross-section of the transuranides has also been studied in this way, with increased precision.

A study on the fission of plutonium 239, by L. Bollinger in which the fission fragments were detected by scintillation in an argon-nitrogen mixture is of interest. A resolution time of 5×10^{-9} s obtained in this

way allowed him to use 120 mg of plutonium in the scintillation chamber; this corresponds to an emission of 3×10^8 α-particles per second. The use of a fast response photomultiplier giving high instantaneous anode currents made it unnecessary to use an amplifier: the discriminator could be connected directly to the output of the photomultiplier.

Other examples of applications of fast response photomultipliers can also be mentioned: the measurement of the neutron flux in critical assemblies and in nuclear reactors which are at the point of going critical; kinetic studies on nuclear reactors by the method of sinusoidal oscillation in an absorbing sample placed in the control-rod system. Finally, mention may be made of γ detection and the study of γ correlation in large accelerators.

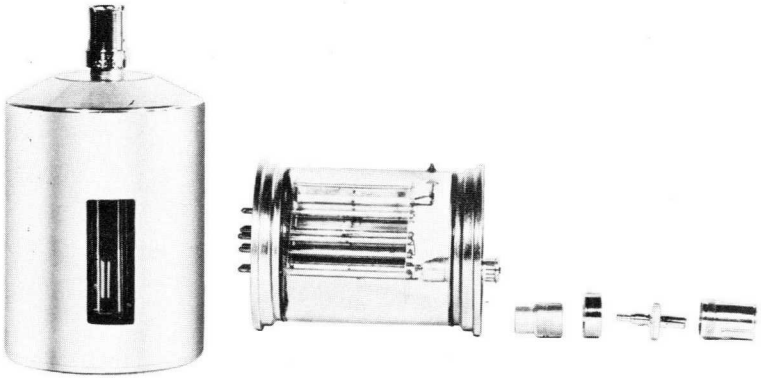

Fast response photomultiplier type XP1143
(approx. 1/3 full size)

7 Detection of Modulated Light by Photomultipliers

The transmission of information by optical carrier waves is the subject of renewed interest at present, largely owing to the appearance of sources of coherent light such as lasers.

The use of light as the carrier wave for information has the following advantages:

- the very high frequencies involved would permit the use of very wide modulation bands, so that information could be transmitted on a *large number of channels* simultaneously. The range of optical frequencies, from $\lambda = 400$ nm to $\lambda = 800$ nm, corresponds to a frequency range of about 4×10^{14} Hz, which is more than enough for all the telecommunication needs which can be though of at the moment.
- for transmission over long distances, the great directivity which can be given to beams of light would also prove very useful. For example, the use of lasers, which are light sources with a high luminance and a very high directivity, has enabled information to be transmitted over distances of several thousand kilometres.

7.1 Optical Receivers

The high directivity of light makes it possible for optical links to be realized over very large distances. However, the maximum range does depend on the sensitivity of the receiver used and on the bandwidth of the signal to be transmitted.

At present, photomultipliers are the most sensitive detectors of light in the visible range. They have the advantage of possessing their own built-in amplifier with a very low noise level, while the sensitivity of a simple photodiode is masked by the noise of the amplifier which follows it.

Photomultipliers as now used for physics applications would make excellent quadratic detectors for modulated light at wavelengths below 650 nm (Sb–Cs cathode, 800 nm (Sb–Na–K–Cs cathode) or 1100 nm (Ag–O–Cs), with modulation frequencies between 0 and about 150 MHz.

A photomultiplier intended for the detection of amplitude-modulated light in a very wide frequency band does not in fact have to meet all the

requirements made on photomultipliers in nuclear physics applications (high gain, large cathode surface area); but it does have to have its own special characteristics, mainly in connection with the need for as wide a passband as possible.

7.2 Sensitivity Limit of Photomultipliers for Modulated Light

In general, the sensitivity of a receiver is limited by noise. In optical receivers such as photomultipliers, the sensitivity is limited simultaneously by:

- the noise (dark current) of the receiver itself;
- the noise due to the quantized nature of the light emitted (Schottky effect).

We have seen that the dark current in phototipliers is partly due to thermionic emission from the photocathode and the dynodes. This thermionic emission can be much reduced by cooling the photomultiplier to such a low temperature that the energy possessed by the thermal electrons is less than the work function of the material.

The quantum noise, on the other hand, cannot possibly be eliminated. It is due to the fluctuations in the mean number of photons reaching the photocathode in a given time. We shall now calculate the ultimate limit of the sensitivity of the detector, i.e. that due the quantized nature of light only.

Let us consider a signal occupying a frequency band of width Δf, which modulates the amplitude of a light wave of frequency ν. The integration time τ of the signal between two consecutive independent values is of the order of:

$$\tau = \frac{1}{2\Delta f}. \tag{12}$$

This time should be less than or equal to the resolution time of the receiver if the information contained in the signal is to be detected without distortion.

The mean number of photons reaching the photomultiplier during the time τ is equal to:

$$\overline{N}_p = \frac{P\tau}{h\nu},$$

where P is the light power applied to the photocathode, in watts.

If η_q is the quantum efficiency of the photocathode, the mean number of useful photons, $\overline{N}'_p$, is equal to:

$$\overline{N}'_p = \eta_q \frac{P\tau}{h\nu}. \tag{13}$$

If we assume that the real number of photons emitted has a normal distribution, then the standard deviation of the above number is:

$$\sqrt{\overline{N}'_p} = \sqrt{\eta_q \frac{P\tau}{h\nu}}. \tag{14}$$

With the aid of equation (12), we find for the corresponding noise power:

$$P \frac{\sqrt{\overline{N}'_p}}{\overline{N}'_p} = \sqrt{\frac{2Ph\nu\Delta f}{\eta_q}}.$$

At the output of a detector with a quadratic characteristic, the power of the electrical signal is proportional to P^2 (with 100% modulation), and the noise power is proportional to:

$$\frac{2\,Ph\nu\Delta f}{\eta_q}. \tag{15}$$

This noise is shot noise (Schottky noise) associated with the continuous component I of the photoelectric current produced by the modulated light. Now since:

$$I^2 = \left(\frac{\overline{N}_p \eta_q e}{\tau}\right)^2 \text{is proportional to } P^2 = \left(\frac{\overline{N}_p h\nu}{\tau}\right)^2,$$

whence

$$\frac{2\,Ph\nu\Delta f}{\eta_q} = k\,(2\,Ie\Delta f),$$

where k is a constant of proportionality.

With the aid of equation (15), we can now write for the signal-to-noise ratio:

$$\frac{P}{2\,\frac{h\nu\Delta f}{\eta_q}}. \tag{16}$$

This ratio has been calculated on the assumption that the light wave is 100% modulated. In the more frequently occurring case where the modulation percentage m is less than 100, the signal-to-noise ratio becomes:

$$\frac{\left(\frac{m}{100}\right)^2 P}{2\,\frac{h\nu\Delta f}{\eta_q}}. \tag{17}$$

With the aid of this expression, we can calculate the minimum light power reaching the receiver needed to give a given signal-to-noise ratio; the intrinsic noise of the receiver has not been taken into consideration here.

7.3 Passband

The passband of a photomultiplier extends from d.c up to a certain cut-off frequency determined by the fluctuations in the transit time of the electrons at the various stages of the tube, by the duration of the currents induced by the electrons in the last few stages of the multiplier and by the time constants of the various inter-electrode connections. For most of the photomultipliers, the 3 dB cut-off frequency lies at about 100 MHz. The type 1210, on the other hand, has a cut-off frequency of about 200 MHz.

The passband can be calculated in a fairly simple manner. Let us suppose that the pulse response of a photomultiplier is represented by a normal distribution of standard deviation σ:

$$R(t) = \exp(-t^2/2\sigma^2)$$

The frequency response will then be:

$$G(\omega) = \int_{-\infty}^{+\infty} R(t) \exp(-j\omega t)\mathrm{d}t$$

$$= \sqrt{2\pi}\,\sigma \exp(-\omega^2\sigma^2/2)$$

Under these conditions, calculation shows that the 3 dB passband is equal to $(0.13)/\sigma$, which comes to 130 MHz for the XP 1020, for which $\sigma = 1$ ns.

Table 3. Principal Characteristics of Fast Response Photomultipliers

type [1]	diameter of photocathode (mm) [2]	no. of stages	spectral response [3]	mean sensitivity of photocathode: to white light (μA/lm) [4]	mean sensitivity of photocathode: to monochromatic light (mA/W) [5]	anode sensitivity: gain at HT voltage (V)	
56 AVP		14	A (S 11)	65	55	10^8	2200
56 CVP		10	C (S 1)	25	2	100 [8]	2750
56 DVP		14	D	—	75	10^8	2300
56 DUVP	42	14	DU	—	75	10^8	2300
56 TVP		14	T (S 20)	115	65	10^8	2500
56 TUVP		14	TU	115	65	10^8	2500
56 UVP		14	U (S 13)	65	55	10^8	2200
58 AVP		14	A (S 11)	70	60	10^8	2400
58 DVP		14	D	—	60	10^8	2400
58 UVP	110	14	U (S 13)	70	60	10^8	2400
XP 1040		14	A (S 11)	70	60	10^8	2400
XP 1041		14	D	—	60	10^8	2400
XP 1020		12	A (S 11)	65	55	10^8	2500
XP 1021		12	A (S 11)	65	55	10^8	2500
XP 1023	42	12	U (S 13)	65	55	10^8	2500
XP 1210		10	A (S 11)	50	40	10^7	4000
XP 1143	opaque cathode	6	S 4	45	40	10^4	3500

[1]) The XP 1020 and XP 1021 only differ in their output impedances, which are 100 Ω for the XP 1020 and 50 Ω for the XP 1021.
[2]) For the XP 1143, the minimum useful area of the photocathode is 7×40 mm^2.
[3]) See the corresponding spectral response curves of Fig. 2.2.
[4]) Measured with the aid of a tungsten-ribbon lamp with a colour temperature of 2854° K.
[5]) Measured at 420 nm (for the C(S_1) types, at 800 nm).

type	dark current,		speed characteristics			linearity		maximum values	
	mean value (max) (μA) [6]	for gain of	transit time (ns) [7]	rise time (ns) [7]	transit-time difference (ns)	high gain (mA) voltage distribution A	high current (mA) voltage distribution B	HT supply voltage (V)	mean anode current (mA)
56 AVP	0.5 (< 5)	10^8	36	2	< 0.5	100	300	2500	0.2
56 CVP	< 10	20 [8]	—	2	< 0.7	—	—	3000	0.03
56 DVP	0.2 (< 1)	10^8	36	2	< 0.5	100	300	2500	0.2
56 DUVP	0.2 (< 1)	10^8	36	2	< 0.5	100	300	2500	0.2
56 TVP	< 5	10^8	36	2	< 1	100	300	2750	0.2
56 TUVP	< 5	10^8	36	2	< 1	100	300	2750	0.2
56 UVP	0.5 (< 5)	10^8	36	2	< 0.5	100	300	2500	0.2
58 AVP	2 (< 12)	10^8	45	2	1	100	300	3000	0.2
58 DVP	2 (< 12)	10^8	45	2	1	100	300	3000	0.2
58 UVP	2 (< 12)	10^8	45	2	1	100	300	3000	0.2
XP 1040	2 (< 12)	10^8	45	2	1	100	300	3000	0.2
XP 1041	2 (< 12)	10^8	45	2	1	100	300	3000	0.2
XP 1020	(< 5)	10^8	28	< 1.8	< 0.2	100	300	3500	0.2
XP 1021	(< 5)	10^8	28	< 1.8	< 0.2	100	300	3000	0.2
XP 1023	(< 5)	10^8	28	< 1.8	< 0.2	100	300	3000	0.2
XP 1210	0.7 (< 1)	10^7	20	1	< 0.2	—	75	5000	—
XP 1143	1 (< 6)	10^4	10	< 1		—	5000	7500	0.2

[6]) Measured at a temperature of 20° C.

[7]) For a light pulse of negligible duration (from spark generator SL 109) illuminating the entire photocathode.

[8]) This value is the anode sensitivity in A/lm.

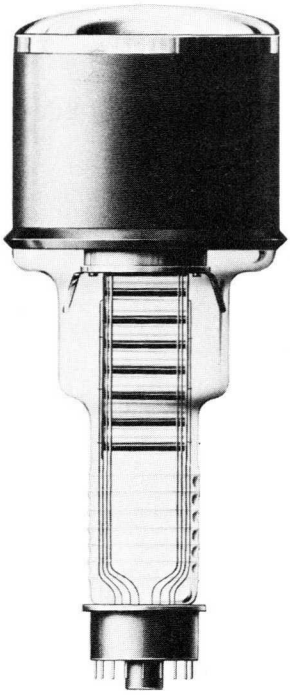

Fast response photomultiplier type 58UVP
(approx. 1/4 full size)

Appendix 1

Mathematical Treatment of Gain Fluctuations

In the problems related to the gain fluctuations in the multiplier, with which we are concerned here, the statistical variables to be dealt with can only assume values equal to positive whole numbers or zero, since the variables in question represent numbers of electrons.

Let us therefore consider a statistical variable s, which may assume a value equal to a positive whole number or zero, with the probability distribution $P(s)$.

We shall define the generating function of this distribution as a function of the auxiliary variable u given by the relation:

$$G(u) = \sum_{s=0}^{\infty} P(s)\, u^s .$$

The mean value of the statistical variable (first-order moment) $\bar{s}$ and its variance (second-order moment) σ^2 are given by:

$$\bar{s} = G'(u), \quad \text{where} \quad u=1 \tag{1}$$

$$\sigma^2 = G''(u) + G'(u) - [G'(u)]^2, \quad \text{where} \quad u=1 . \tag{2}$$

Let us now consider a random event with only one alternative, between $s=0$ and $s=1$. This is the case in photoelectric emission, where a photon has a probability η_q of liberating an electron, and a probability $(1-\eta_q)$ of not doing so. For this case, the generating function may be written:

$$G(u) = (1-\eta_q) + \eta_q u.$$

It follows from equations (1) and (2) that the mean value and the variance in this case are:

$$\bar{s} = \eta_q, \tag{3}$$

$$\sigma^2 = \eta_q (1-\eta_q) . \tag{4}$$

We shall now show that the generating function for the electron distribution at the output of a photomultiplier can easily be calculated from the generating functions of the successive statistical events involved in the operation of the detector. The mean number of electrons at the output, and

the variance of this value, can thus be related to the moments characterizing these elementary statistical events.

We shall now go through the various stages of conversion and amplification occurring in a photomultiplier, with this aim in view.

Photoelectron conversion

If only one basic event out of a certain set of random events A, B, ... can occur in a given experiment, and if the probability of occurrence of the different events in successive experiments is given by $P(A)$, $P(B)$, ... respectively, then the generating function of the composite event is given by the *weighted mean* of the generating functions $A(u)$, $B(u)$, ... of the component events:

$$G(u) = P(A)\,A(u) + P(B)\,B(u) + \ldots \tag{5}$$

Let us consider the photoelectron conversion produced by the cathode as an example. The photocathode will not in general have exactly the same photoelectric sensitivity at all points on its surface. We may thus divide the heterogeneous surface of the photocathode into a sufficient number n of elementary zones of equal area, zone i being associated with a probability of photoelectric emission η_{qi}. The arrival of a photon in zone i (with a probability $P(i)$) thus constitutes and elementary event, represented by the generating function:

$$A_i(u) = (1-\eta_{qi}) + \eta_{qi}u.$$

The generating function for the cathode as a whole will thus be:

$$G(u) = \sum_{i=0}^{n} P(i)[(1-\eta_{qi}) + \eta_{qi}\,u].$$

If the illumination is uniform, i.e. if the photon has the same probability of falling on any of the elementary zones, then we have:

$$P(1) = P(2) = \ldots P(n) = \frac{1}{n},$$

and in this case:

$$G(u) = \frac{1}{n}\sum_{i=0}^{n}[(1-\eta_{qi}) + \eta_{qi}u].$$

The mean number of electrons emitted by an arbitrary point on the catho-

de struck by a single photon and the variance σ^2 of this value, can thus be calculated from equations (1) and (2). This gives:

$$\bar{N}_{ei} = \frac{1}{n} \sum_{i=0}^{n} \eta_{qi} = \bar{\eta}_q \tag{6}$$

and

$$\sigma_e^2 = \bar{\eta}_q (1 - \bar{\eta}_q), \tag{7}$$

where $\bar{\eta}_q$ is the mean quantum efficiency of the photocathode.

Conversion of N_p photons

When a number of random events, from a set of independent events A, B, ... occur simultaneously, the generating function of the new statistical variable is:

$$G(u) = A(u)\, B(u) \ldots$$

It follows that if N_p photons arrive simultaneously at the photocathode, the generating function associated with the sum of these N_p independent events is:

$$G(u) = [(1 - \bar{\eta}_q) + \bar{\eta}_q u]^{N_p} .$$

The mean number of electrons emitted, and the variance of this value, are thus:

$$\bar{N}_e = N_p \bar{\eta}_q \quad \text{and} \quad \sigma^2 = N_p \bar{\eta}_q (1 - \bar{\eta}_q) . \tag{8}$$

Note: Strictly speaking, we should have written:

$$G(u) = \left\{ \frac{1}{n} \sum_{i=0}^{n} [(1 - \eta_{qi}) + \eta_{qi} u] \right\}^{N_p} ,$$

but this leads to the same result.

Electron multiplication

The electron multiplication occurring from dynode to dynode in the multiplier can be considered to a first approximation as a series of events "in cascade". Let us consider two successive dynodes (S1) and (S2) of the multiplier. If dynode (S1) emits a group of N_e electrons (event 1), the secondary emission of dynode (S2) (event 2) on receipt of these N_e

"primary" electrons may be regarded as the sum of N_e identical, independent events; this is what we mean when we say that events (1) and (2) are in cascade.

In this case, if $B(u)$ is the generating function associated with the statistical distribution of the secondary electrons emitted by dynode (S2) when struck by a single "primary" electron, and $A(u)$ is the corresponding generating function for dynode (S1), then it can be shown that the generating function associated with the total number of electrons emitted by dynode (S2) is:

$$G(u) = A[B(u)] . \tag{9}$$

The mean value of the statistical variable s may now be calculated with the aid of equation (1). This gives:

$$\bar{s} = \bar{s}_A \cdot \bar{s}_B , \tag{10}$$

where $\bar{s}_A$ and $\bar{s}_B$ are the mean values of the statistical variables associated with events A and B.

The variance can now be calculated with the aid of equation (2):

$$\sigma^2 = \bar{s}_B^2 \sigma_A^2 + \bar{s}_A \sigma_B^2 .$$

In general, it is more useful to consider the relative variance $\upsilon = \sigma^2/\bar{s}^2$. In the present case, we find for this:

$$\upsilon = \upsilon_A + \frac{\upsilon_B}{\bar{s}_A} . \tag{11}$$

If the multiplier has a total of n dynodes, then by repeating the above process we arrive at the following expression for the mean number of electrons $\overline{N}_e$ produced at the output of the multiplier when a single photoelectron enters the input:

$$\overline{N}_e = \overline{N}_{e1} \cdot \overline{N}_{e2} \ldots \overline{N}_{en} \tag{12}$$

while the corresponding relative variance may be written:

$$\upsilon_e = \upsilon_{e1} + \frac{\upsilon_{e2}}{\overline{N}_{e1}} + \frac{\upsilon_{e3}}{\overline{N}_{e1}\overline{N}_{e2}} + \ldots \frac{\upsilon_{en}}{\overline{N}_{e1}\overline{N}_{e2} \ldots \overline{N}_{en-1}} . \tag{13}$$

Now the mean values $\overline{N}_{e1}$, $\overline{N}_{e2}$, ... are in fact the interstage gains of the multiplier, and therefore, we may write:

$$\overline{N}_{ei} = \bar{\eta}_{ci} \cdot \bar{\delta}_i$$

where $\bar{\delta}_i$ is the mean secondary-emission coefficient of the i^{th} dynode and $\bar{\eta}_{ci}$ is the mean collection efficiency between this dynode and the next.

The relative variance of the real gain of the multiplier thus becomes:

$$\upsilon_{G_r} = \upsilon_{g_1} + \frac{\upsilon_{g_2}}{\eta_{c1}\delta_1} + \frac{\upsilon_{g_3}}{\eta_{c1}\delta_1 \cdot \eta_{c2}\delta_2} + \ldots \frac{\upsilon_{gn}}{\eta_{c1}\delta_1 \cdot \eta_{c2}\delta_2 \ldots \eta_{cn-1}\delta_{n-1}} . \tag{14}$$

Appendix 2

Calculation of Relative Variance of Electron Distribution at the Output of a Scintillation Detector

(after the theory developed by E. Breitenberger)

When radiation strikes a scintillation detector, it is only the mean quantity Q of charge appearing at the output of the detector which is proportional to the energy of the incident radiation. The value of Q is subject to statistical variations of which we now propose to calculate the relative variance v_Q.

We start making the simplifying assumption that each particle of the incident radiation gives up the same amount of energy to the scintillator, and this constant amount of energy yields a variable number of photons (event X). We assume further that each photon emitted has a certain probability of reaching the photocathode (event T).

The emission of the photons by the scintillator (X), their transfer (T) to the photocathode and the conversion of the photons into output electrons (event M) may thus be regarded as a series of events in cascade.

Let us denote the generating functions associated with these three events by $X(u)$, $T(u)$ and $M(u)$ respectively.

Analogous to equations (12) and (13), the mean value of the variable associated with the resulting generating function $G(Q)$ is:

$$\bar{s}_Q = \bar{s}_X \cdot \bar{s}_T \cdot \bar{s}_M$$

and the relative variance

$$v_Q = v_X + \frac{v_T}{\overline{X}} + \frac{v_M}{\overline{X}\,\overline{T}} \tag{15}$$

where v_X, v_T and v_M are the relative variances associated with the generating functions $X(u)$, $T(u)$ and $M(u)$ and:

$$\overline{N}_p = \overline{X} \cdot \overline{T}$$

is the mean number of photons arriving at the photocathode. If v_p is the relative variance of this number we can simplify (15) very appreciably with the aid of (11)

$$v_Q = v_p + \frac{v_M}{\overline{N}_p} \tag{16}$$

where:

$$v_p = v_X + \frac{v_T}{\bar{X}} \tag{17}$$

On the other hand, the relative variance v_M associated with the photon-electron conversion in the photomultiplier may be written in terms of the three main measurable parameters of the photomultiplier, viz. the quantum efficiency η_q of the photocathode, the overall collection efficiency η_c and the relative variance v_s of the multiplier, calculated from the single-electron spectrum (see 3.3.1).

Detection, collection and multiplication can also be considered as three events A, B and C in cascade. The overall relative variance associated with these three events can thus be written (with equation (13)):

$$v_M = v_{\eta_q} + \frac{v_{\eta_c}}{\eta_q} + \frac{v_s}{\eta_c \eta_q},$$

where v_{η_q} and v_{η_c} are:

$$v_{\eta_q} = \frac{\sigma_{\eta_q}^2}{\eta_q^2} = \frac{1-\eta_q}{\eta_q}, \text{ and } v_{\eta_c} = \frac{\sigma_{\eta_c}^2}{\eta_c^2} = \frac{1-\eta_c}{\eta_c}.$$

It follows that:

$$v_M = \frac{1+v_s}{\eta_c \eta_q} - 1$$

and substituting this expression in (16), we find:

$$v_Q = v_p - \frac{1}{\bar{N}_p} + \frac{1+v_s}{\bar{N}_p \eta_c \eta_q}$$

or

$$v_Q = v_p + \frac{1-\eta_c \eta_q + v_s}{\bar{N}_p \eta_c \eta_q}. \tag{18}$$

Appendix 3

Calculations Concerning Time Fluctuations
(after the theory developed by E. Gatti)

Relative variance of the width of the anode pulse
Consider two successive dynodes of the multiplier; and let us suppose that a group of N_e electrons leaves the first of these dynodes at the same moment. (We may imagine, if we wish, that these N_e electrons all come from the secondary emission produced when one single electron falls on the first dynode.)

These N_e electrons will reach the second dynode at different moments. If τ_i is the difference between the time of arrival of the i^{th} electron and the mean time of arrival, the width ψ_A of the pulse formed by the N_e electrons on arrival at the second dynode is defined as:

$$\psi_A^2 = \sigma_{SS}^2 = \frac{\sum_{i=1}^{N_e} \tau^2}{N_e} \tag{19}$$

Differentiating with respect to τ_i, we find:

$$\psi_A \mathrm{d}\psi_A = \frac{\sum_{i=1}^{N_e} \tau_i \mathrm{d}\tau_i}{N_e}$$

or, bearing in mind the general relation:

$$\sigma_f^2 = \left(\frac{\delta f}{\delta \alpha_1}\right)^2 \sigma_{\alpha_1}^2 + \left(\frac{\delta f}{\delta \alpha_2}\right)^2 \sigma_{\alpha 2}^2 + \ldots + \left(\frac{\delta f}{\delta \alpha_n}\right)^2 \sigma_{\alpha_n}^2 \tag{20}$$

where f is a function of the independent variables $\alpha_1, \alpha_2, \ldots \alpha_n$, we find for the variance of the width of the pulse produced by the arrival of the N_e electrons at the second dynode:

$$\sigma_{\psi_A}^2 = \sum_{i=1}^{N_e} \left(\frac{\delta \psi_A}{\delta \tau_i}\right)^2 \sigma_{\tau_i}^2 = \frac{\sigma_{SS}^2}{N_e} \tag{21}$$

where σ_{SS}^2 is the variance of the difference in transit times τ_i between the two dynodes in question.

After these N_e electrons have been multiplied by secondary emission, the pulse width becomes:

$$\psi_B^2 = \frac{\sum_{i=1}^{N_e} g_i \tau_i^2}{\sum_{i=1}^{N_e} g_i} \tag{22}$$

where g_i represents the gain of the stage for the i^{th} electron (g_i and τ_i uncorrelated variables). We may consider, on the average, that multiplication does not broaden the pulse, i.e.:

$$\psi_A^2 = \psi_B^2 .$$

Differentiating (22) with respect to g_i and τ_i and bearing the general relation (20) in mind, we find for the variance of the pulse width after multiplication of the electrons:

$$\sigma_{\psi_B}^2 = \frac{\sum_{i=1}^{N_e} (\tau_i^2 - \psi_B^2)^2}{4\,\psi_B^2 N_e^2 g^2}\,\sigma_g^2 + \frac{\sum_{i=1}^{N_e} g_i^2 \tau_i^2}{\psi_B^2 N_e^2 g^2}\,\sigma_{SS}^2 \tag{23}$$

where σ_g^2 is the variance of the gain of the stage and:

$$N_e g = \sum_{i=1}^{N_e} g_i .$$

We now assume that the inter-dynode transit-time differences τ_i have a Gaussian distribution, normalized so that the total area under the curve is N_e, i.e.:

$$\mathrm{d}P(\tau_i) = \frac{N_e}{\sigma_{SS}\sqrt{2\pi}} \exp\left(-\frac{\tau_i^2}{2\sigma_{SS}^2}\right)\mathrm{d}\tau_i .$$

We can now calculate the first term on the right-hand side of (23), making use of the approximation:

$$\sum_{i=1}^{N_e} \tau_i^4 = \int_{-\infty}^{+\infty} \tau_i^4 \,\mathrm{d}P(\tau_i) = 3\,N_e \sigma_{SS}^4 .$$

In the second term on the right-hand side of (23), we have:

$\sum_{i=1}^{N_e} g_i^2 \tau_i^2 = N_e \sigma_{SS}^2 (g^2 + \sigma_g^2)$. Equation (23) then becomes

$$\sigma_{\psi_B}^2 = \frac{\sigma_{SS}^2}{N_e}\left(1 + \frac{3}{2}\frac{\sigma_g^2}{g^2}\right) = \frac{\sigma_{SS}^2}{N_e}\left(1 + \frac{3}{2}\upsilon_g\right) \tag{24}$$

where υ_g is the relative variance of the gain of the stage.

As the multiplication of the electrons does not, on the average, change the width of the pulse ($\psi_A^2 = \psi_B^2$), we can simply calculate the width of the pulse after n multiplications in cascade from:

$$\psi^2 = \sum_{i=2}^{n+1} \psi_i^2 = n\sigma_{SS}^2 \tag{25}$$

Let us now calculate the variance σ_ψ^2 of ψ. For this purpose, we differentiate (25):

$$\psi \mathrm{d}\psi = \sum_{i=2}^{n+1} \psi_i \mathrm{d}\psi_i$$

whence:

$$\psi^2 \sigma_\psi^2 = \sum_{i=2}^{n+1} \psi_i \sigma_{\psi_i}^2 = \sigma_{SS}^2 \sum_{i=2}^{n+1} \sigma_{\psi_i}^2 .$$

With the aid of (24), this becomes:

$$\psi^2 \sigma_\psi^2 = \sigma_{SS}^4 \left(1 + \frac{3}{2}\upsilon_g\right) \sum_{i=2}^{n+1} \frac{1}{N_{ei}}$$

On the average, we may take:

$N_{e2} = g$, $N_{e3} = g^2$, etc.

This gives (since $g > 1$):

$$\psi^2 \sigma_\psi^2 = \frac{\sigma_{SS}^4}{g-1}\left(1 + \frac{3}{2}\upsilon_g\right).$$

Combining this with (25), we find for the relative variance of the pulse width:

$$v_\psi = \frac{\sigma_\psi^2}{\psi^2} = \frac{1}{(g-1)n^2}\left(1+\frac{3}{2}v_g\right). \tag{26}$$

Putting $v_g = 1/g$, we can also write the relative variance of ψ in the form:

$$v_\psi = \frac{1}{(g-1)n^2}\left(1+\frac{3}{2g}\right). \tag{27}$$

Variance of the position of the centre of gravity of the pulse on the time axis

We shall now calculate the variance of the time between the emission of a photoelectron and the arrival of the centre of gravity of the corresponding pulse in the anode circuit, by a method similar to that used above.

The centre of gravity of a pulse starting from one dynode is defined by:

$$\chi_B = \frac{\sum_{i=1}^{N_e} g_i\tau_i}{\sum_{i=1}^{N_e} g_i}. \tag{28}$$

Differentiating with respect to τ_i and g_i, and considering that the mean value of the numerator of (28) is zero, we find:

$$\mathrm{d}_{\chi_B} = \frac{\sum_{i=1}^{N_e} (g_i\,\mathrm{d}\tau_i + \tau_i\,\mathrm{d}g_i)}{\sum_{i=1}^{N_e} g_i}$$

from which we deduce the variance $\sigma_{\chi_B}^2$, with the aid of the general relation

$$\sigma_{\chi_B}^2 = \sum_{i=1}^{N_e}\left[\left(\frac{\delta\chi_B}{\delta\chi_i}\right)^2\sigma_{SS}^2 + \left(\frac{\delta\chi_B}{\delta g_i}\right)^2\sigma_g^2\right],$$

whence

$$\sigma_{\chi_B}^2 = \frac{\sum_{i=1}^{N_e} [g_i^2 \sigma_{SS}^2 + \tau_i^2 \sigma_g^2]}{\sum_{i=1}^{N_e} g_i} .$$

We now make use of the approximations:

$$\sum_{i=1}^{N_e} g_i = N_e g \text{ and } \sum_{i=1}^{N_e} g_i^2 = N_e(g^2 + \sigma_g^2)$$

and, with the aid of (19), we find:

$$\sigma_{\chi_B}^2 = \frac{\sigma_{SS}^2}{N_e}\left(1 + \frac{2\sigma_g^2}{g^2}\right) = \frac{\sigma_{SS}^2}{N_e}(1+2\upsilon_g) \tag{29}$$

where υ_g is the relative variance of the gain per stage:

σ_g^2/g^2 .

The variance of the time at which the centre of gravity of the pulse occurs, for the photomultiplier as a whole, is thus:

$$\sigma_\chi^2 = \sigma_{CS1}^2 + \sum_{i=2}^{n+1} \frac{\sigma_{SS}^2}{N_{ei}}(1+2\upsilon_g) .$$

Again taking:

$N_{e2} = g$ and $N_{e3} = g^2$,

we find

$$\sigma_\chi^2 = \sigma_{CS1}^2 + \frac{\sigma_{SS}^2}{g-1}(1+2\upsilon_g) \tag{30}$$

where σ_{CS1}^2 is the variance of the transit time between the cathode and the first dynode, and σ_{SS}^2 is the variance in transit time between two successive dynodes.

If we again put $\sigma_g^2 = g$ and $\upsilon_g = 1/g$, as above, we can finally write equation (30) in the form:

$$\sigma_\chi^2 = \sigma_{CS1}^2 + \frac{\sigma_{SS}^2}{g-1}\left(1 + \frac{2}{g}\right). \tag{31}$$

Fast response photomultiplier type 58AVP
(approx. 1/3 full size)

Appendix 4

Spark Generator type SL 109

Spark generator type SL 109 is a source of light pulses of extremely short duration. It is intended for investigation of the speed of photomultipliers and associated circuitry. The half-height width of the light pulses is less than one nanosecond, and these pulses can be produced either one at a time or at regular intervals at frequencies of up to 150 pulses per second. The light pulses are produced by discharge of a capacitor between a point electrode and a spherical electrode in air.

The capacitor is charged to a variable voltage between 3500 and 5000 V and is discharged via the spark gap and a thyratron which is made temporarily conducting by a triggering pulse applied to the cathode. Normally, this tube is kept cut off by a positive voltage of 50–150 V applied to the cathode.

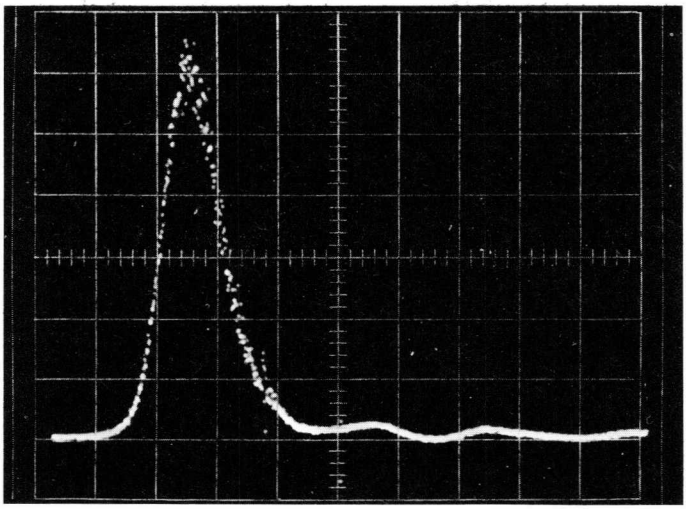

Fig. A4.1. The light pulse emitted by the spark generator SL 109, as detected by an AVHC 41 diode and observed on a sampling oscilloscope.
Ordinate scale: 70 mV per main division.
Abscissa scale: 1 ns per main division.

The light pulse produced between the electrodes of the spark gap is intense enough to be observed by a photoelectric cell with plane parallel electrodes (type AVHC 40 or AHVC 41, for example), the relatively short rise time of which (of the order of a few tenths of a nanosecond) allows the form of the pulse to be faithfully reproduced. The oscillogram in Fig. A4.1 shows the form of the light pulse, determined in this way.

An electrical synchronization signal may be taken from the ends of a 50 Ω matched load inserted in the discharge circuit of the capacitor.

The triggering pulse comes from a relay with mercury-wetted electrodes, and is given the desired form by a coaxial line. The amplitude of this pulse may vary from 100 to 500 V.

The pulse generator SL 109 is built in two units:

- one contains the light-pulse source proper, with the triggering circuit and the photoelectric cell for checking the pulse;
- the other contains the HT supply and the circuits which supply the triggering signal.

Bibliography

1. Boutry G. A. – Physique appliquée à l'Industrie du Vide et de l'Electronique, Masson-Paris 1962.
2. Breitenberger E. – Scintillation spectrometer statistics, Prog. Nucl. Phys., 4, 56–94, 1955.
3. Gatti E., Svelto V. – Theory of time resolution in scintillation counters. Nucl. Inst. and Meth., 4.1, 189–201, 1959.
4. Pietri G. – Les photomultiplicateurs, instruments de physique expérimentale. Acta Electronica, 5.1, 7–30, 1961.
5. Pietri G. – Present state of research and new developments at the "Laboratoires d'électronique et de physique appliquées" in the field of multiplier tubes. IEEE Trans. Nucl. Sci., NS 11, 76–91, June, 1964.
6. Evrard R., Gazier C. – Propriétés statistiques de certain photomultiplicateurs, 56AVP, XP1020. J. Phys., 26.1, 37A–48A, 1965.
7. Barbier M. – Conception d'un photomultiplicatuer à réponse rapide. Acta Electronica, 5.1, 31–38, 1961.
8. Gazier C. – Contribution à l'étude des propriétés statistiques du gain du photomultiplicatuer. Thèse d'ingénieur du C.N.A.M., 1963.
9. Pietri G. – Progress in photomultiplier tubes for scintillation counting and nuclear physics. IRE Trans. Nucl. Sci., NS9, no. 3, 62–72, June 1962.
10. Pietri G., Nussli J., Brault M. – Perfectionnements récents apportés aux photomultiplicateurs rapides destinés à la physique nucléaire, Nov. 1963.
11. Marcy R., Marguin J. – Statistiques des photoélectrons d'un photomultiplicateur éclaire en luminière cohérente et incohérente. L'onde Electrique, t. XLV, pp. 1102–1109, Septembere 1965.
12. Billard P., Donjon J., Marie G. – Application de la modulation de lumière aux télécommunications, Acta Electronica, 9.4, 305–313, 1965.
13. Nussli J. – Aperçu sur les possibilités offertes par les photomultiplicateurs rapides dans la détection de lumière modulée "Electronique quantique, comptes rendus de la 3e conférence internationale" Dunod, Paris, t. 2, pp. 1723–1730.
14. La Radiotechnique-Compelec. – Les tubes photomultiplicateurs. Brochure éditée par la Radiotechnique-Compelec. 2e édition. April 1965.
15. Schonkeren J. M. – Photomultipliers. Application Book by N.V. Philips Gloeilampenfabrieken, Elcoma Division, April 1970.

Technology relating to the products described in this book is shared by the following companies.

Argentina
FAPESA I.y.C.
Melincué 2594
Tel. 50-9941/8155
BUENOS AIRES

Australia
Philips Industries Ltd.
Miniwatt Electronics Division
20, Herbert St.
Tel. 43-2171
ARTARMON, N.S.W.

Austria
WIVEG
Zieglergasse 6
Tel. 93 26 22
A1072 VIENNA

Belgium
M.B.L.E.
80, rue des Deux Gares
Tel. 23 00 00
1070 BRUSSELS

Brazil
IBRAPE S.A.
Rua Manoel Ramos Paiva 506
Tel. 93-5141
SAO PAULO

Canada
Philips Electron Devices
116 Vanderhoof Ave.
Tel. 425-5161
TORONTO 17, Ontario

Chile
Philips Chilena S.A.
Av. Santa Maria 0760
Tel. 39 40 01
SANTIAGO

Colombia
SADAPE S.A.
Calle 19, No. 5-51
Tel. 422-175
BOGOTA D.E. 1

Denmark
Miniwatt A/S
Emdrupvej 115A
Tel. (01) 69 16 22
DK-2400 KØBENHAVN NV

Finland
Oy Philips A.B.
Elcoma Division
Kaivokatu 8
Tel. 10 915
HELSINKI 10

France
R.T.C.
La Radiotechnique-Compelec
Avenue Ledru Rollin 130
Tel. 357-69-30
PARIS 11

Germany
VALVO G.m.b.H.
Valvo Haus
Burchardstrasse 19
Tel. (0411) 3296-1
2 HAMBURG 1

Greece
Philips S.A. Hellénique
Elcoma Division
52, Av. Syngrou
Tel. 915.311
ATHENS

Hong Kong
Philips Hong Kong Ltd.
Components Deps.
St. George's Building 21st Fl.
Tel. K-42 82 05
HONG KONG

India
INBELEC Div. of
Philips India Ltd.
Band Box Building
254-D, Dr. Annie Besant Road
Tel. 45 33 86, 45 64 20, 45 29 86
Worli, BOMBAY 18 (WB)

Indonesia
P.T. Philips-Ralin Electronics
Elcoma Division
Djalan Gadjah Mada 18
Tel. 44 163
DJAKARTA

Ireland
Philips Electrical (Ireland) Pty.
Newstead, Clonskeagh
Tel. 69 33 55
DUBLIN 6

Italy
Philips S.p.A.
Sezione Elcoma
Piazza IV Novembre 3
Tel. 69.94
MILANO

Japan
NIHON PHILIPS
32nd Fl., World Trade Center
Bldg. 5, 3-chome. Shiba
Hamamatsu-cho
Minato-ku
Tel. (435) 5204-5
TOKYO

Mexico
Electrónica S.A. de C.V.
Varsovia No. 36
Tel. 5-33-11-80
MEXICO 6, D.F.

Netherlands
Philips Nederland N.V.
Afd. Elonco
Boschdijk, VB
Tel. (040) 433 33 33
EINDHOVEN

New Zealand
EDAC Ltd.
70-72 Kingsford Smith Street
Tel. 873 159
WELLINGTON

Norway
Electronica A/S
Middelthunsgate 27
Tel. 46 39 70
OSLO 3

Peru
CADESA
Jr. Ilo, No. 216
Appartado 10132
Tel. 27 73 17
LIMA

Portugal
Philips Portuguesa S.A.R.L.
Rua Joaquim Antonio de
Aguiar 66
Tel. 68 37 21/9
LISBOA

South Africa
EDAC (Pty) Ltd.
South Park Lane
New Doornfontein
Tel. 24/6701-2
JOHANNESBURG

Spain
COPRESA S.A.
Balmes 22
Tel. 2 32 66 80
BARCELONA 7

Sweden
ELCOMA A.B.
Lidingövägen 50
Tel. 08/67 97 80
10250 STOCKHOLM 27

Switzerland
Philips A.G.
Edenstrasse 20
Tel. 051/44 22 11
CH-8027 ZUERICH

Taiwan
Philips Taiwan Ltd.
San Min Building, 3rd Fl.
57-1, Chung Shan N. Road
Section 2
Tel. 55 31 01
TAIPEI

Turkey
Türk Philips Ticaret A.S.
EMET Department
Gümüssuyu Cad.78-80
Tel. 45.32.50
Beyoglü, ISTANBUL

United Kingdom
Mullard Ltd.
Mullard House
Torrington Place
Tel. 01-580 6633
LONDON W.C. 1

United States
Amperex Electronic Corp.

Electron Tubes Div.
Tel. 516 WE 1-6200
HICKSVILLE N.Y.

Sem. and Microcircuits Div.
Tel. 401-762-9000
SLATERSVILLE R.I. 02876

Electronic Components Div.
Tel. 516-234-7000
HAUPPAGE N.Y

Ferroxcube Corp.
(Memory Products)
P.O. Box 359
Tel. (914) 246-2811
SAUGERTIES, N.Y. 12477

Uruguay
Luzilectron S.A.
Rondeau 1567, piso 5
Tel. 9 43 21
MONTEVIDEO

Venezuela
C.A. Philips Venezolana
Elcoma Department
Colinas de Bello Monte
Tel. 72.01.51
CARACAS

Printed in The Netherlands 21C33 ③⑤㉒ 9399 246 00101